Science of the Total Environment 967 (2025) 178813

Contents lists available at ScienceDirect

Science of the Total Environment

journal homepage: www.elsevier.com/locate/scitotenv

Modelling oxidative potential of atmospheric particle: A 2-year study over France

Matthieu Vida [a], Gilles Foret [b,*], Guillaume Siour [b], Jean-Luc Jaffrezo [c], Olivier Favez [d,e], Arineh Cholakian [f], Julie Cozic [g], Harry Dupont [g], Grégory Gille [h], Sonia Oppo [h], Shouwen Zhang [i], Florie Francony [j], Cyril Pallares [k], Sébastien Conil [l], Gaelle Uzu [c,*], Matthias Beekmann [a]

[a] Université Paris Cité and Univ Paris Est Creteil, CNRS, LISA, F-75013 Paris, France
[b] Univ Paris Est Créteil and Université Paris Cité, CNRS, LISA, F-94010 Créteil, France
[c] Institut des Géosciences de l'Environnement, IGE, UMR 5001, F-38000 Grenoble, France
[d] Institut National de l'Environnement Industriel et des Risques, INERIS, F-60550 Verneuil-en-Halatte, France
[e] Laboratoire Central de Surveillance de la Qualité de l'air, LCSQA, F-60550 Verneuil-en-Halatte, France
[f] Laboratoire de Météorologie Dynamique (LMD), Ecole Polytechnique, IPSL Research University, Ecole Normale Supérieure, Université Paris-Saclay, Sorbonne Universités, UPMC Université Paris 06, CNRS, Route de Saclay, F-91128 Palaiseau, France
[g] Atmo Auvergne-Rhône-Alpes, F-69500 Bron, France
[h] Atmo Sud, F-13294 Marseille, France
[i] Atmo Hauts de France, F-59044 Lille, France
[j] Atmo Nouvelle Aquitaine, F-33692 Mérignac, France
[k] Atmo Grand Est, F-67300 Schiltigheim, France
[l] ANDRA DISTEC/EES Observatoire Pérenne de l'Environnement, F–55290 Bure, France

HIGHLIGHTS

- Oxidative potential (OP) is as a new metric for air quality.
- We develop and describe a new method to model OP (for AA and DTT assays).
- The simulation of particulate matter and OP is evaluated against observations.
- In France, sources contributing the most to aerosol mass do not have the highest OP.
- Road traffic and biomass burning are often the sources with most OP.

GRAPHICAL ABSTRACT

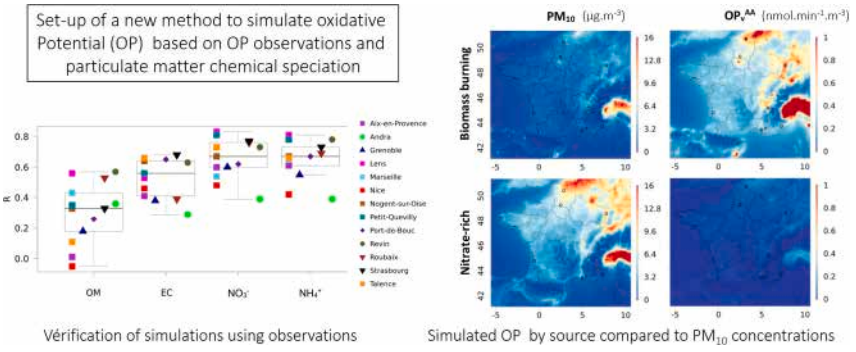

ARTICLE INFO

Editor: Meng Gao

ABSTRACT

The oxidative potential (OP) of particulate matter (PM) has emerged as a promising indicator of the adverse effects of PM on human health. In particular, OP is an indicator for oxidative stress in biological media through formation of reactive oxygen species. To provide a mapping of the spatial and temporal OP variability over

* Corresponding authors.
E-mail addresses: gilles.foret@lisa.ipsl.fr (G. Foret), gaelle.uzu@ird.fr (G. Uzu).

https://doi.org/10.1016/j.scitotenv.2025.178813
Received 5 December 2024; Received in revised form 28 January 2025; Accepted 8 February 2025
Available online 12 February 2025

Keywords:
Atmospheric particles
Air quality
Oxidative potential
Numerical modelling

France, we have developed a strategy to simulate the volume-normalized oxidative potential (OP_v) in the state-of-the-art CHIMERE air quality model over the metropolitan French territory for the years 2013 and 2014. To do so, we combined a measurement-derived and source specific intrinsic OP (OP_i) receptor modelling approach with Particle Source Apportionment Technology (PSAT) in CHIMERE. First, the model's ability to reproduce PM_{10} concentrations and speciation was verified using in situ observations in mainland France. Furthermore, a mostly satisfying correspondence between receptor model and PSAT outputs was obtained considering their source specific chemical profiles. Simulated versus observed OP_v values showed median correlations ranging from 0.35 to 0.60 and mean fractional biases from −30 % to zero, depending on the OP assay considered (ascorbic acid AA, or dithiothreitol DTT) and the PM sources taken into account (i.e. two methods with different PM sources have been used, the reduced and the extended set methods). The modelled two-year average OP_v fields show greater spatial hot spots over large urban areas (especially along roadsides) compared to those for PM_{10} distributions, due to elevated intrinsic OP_i values for the primary anthropogenic sources such as traffic and biomass burning. These effects are stronger for the AA compared to the DTT assays, and for a method with a reduced set compared to an extended set of sources. Overall, through the OP apportionment, these results advocate for reinforcing action plans to reduce emissions from road traffic as well as biomass burning emissions.

1. Introduction

Epidemiological studies have shown that air pollution causes and exacerbates respiratory and cardiovascular diseases while also playing a role in the course of other diseases such as obesity, diabetes or psychotic disorders (Brook et al., 2010; Pignon et al., 2022; Weichenthal et al., 2014). In particular, atmospheric aerosols are considered to have the greatest impact on human health, possibly accounting for about 90 % of the sanitary impact of air pollution (Lelieveld et al., 2015). For instance, in France, it is considered that around 40,000 people die prematurely every year in France because of fine particulate pollution, although Europe is far from the most polluted region in the world (Adélaïde et al., 2020).

In order to reduce the health risks linked to the inhalation of airborne particles, the World Health Organization recommends yearly concentration thresholds of 15 μg m^{-3} and 5 μg m^{-3} for particulate matter with aerodynamic diameter below 10 μm (PM_{10}) and 2,5 μm ($PM_{2.5}$), respectively (WHO, 2021). These drastic thresholds rely solely on the mass concentration of particulate matter (PM), not considering their chemical composition or sources, which can lead to an obvious bias. Indeed, at equal mass concentrations, the aerosol toxicity can be very different, with combustion sources potentially more damaging compared to others (e.g., Park et al. (2018)). Increasing our knowledge on the sources of greater health concern would allow targeting pollutant emission reductions more efficiently. It is therefore vital to search for better indicators of aerosol toxicity rather than looking at particulate mass. With this objective in mind, the PM oxidative potential (OP) has been proposed as a new metric to be considered in air quality monitoring (e.g., Steenhof et al., 2011). Epidemiological studies also indicate that OP may be a relevant indicator of acute effects of aerosols on human health (Bates et al., 2019; Gao et al., 2020). OP is then a promising health-based metric for air quality listed as recommended in the new EU directive 2024/2881/CE.

OP measures the ability of particles to generate oxidative stress in the body induced by exogenous reactive oxygen species (ROS) such as OH, HONO or superoxide ions (Ayres et al., 2008; Cho et al., 2005; Li et al., 2009; Sauvain et al., 2008). When in excess, ROS deplete the lung antioxidants and may lead to imbalance between oxidants and antioxidants. This potentially induces oxidative stress, defined as oxidative damage to any cell material and ultimately inflammation at the origin of biological health endpoints (Costabile et al., 2019; Karavalakis et al., 2017; Steenhof et al., 2011; Weichenthal et al., 2016). The antioxidant depletion can now be measured by spectrophotometry after exposing PM filters into a simulated lung fluid according to different protocols using different lung antioxidants or surrogates such as ascorbic acid (AA) and dithiothreitol (DTT) (Calas et al., 2017). The kinetic depletion rate is then taken as the oxidative potential. To date, there is no clear consensus on which assay – or assay's combination – should be considered as the more relevant indicator, but recent epidemiological studies show that OP_v^{AA} appears to be associated to biomarkers of inflammation (Leni et al., 2020; Marsal et al., 2024) and that OP_v^{DTT} is relevant for various health outcomes (Gao et al., 2020). Collective research efforts are still needed to harmonize protocols to ensure a better consistency among epidemiological studies.

As it is impossible to identify all the chemical species that make up PM and contribute to the OP, an alternative is to use their contributions from sources, which eliminates the need for such detailed knowledge. As previously developed in the China by Liu et al. (2014) and in the USA by Verma et al. (2014), attribution of the OP_v to aerosol sources by a PMF receptor model including uncertainties was pioneered in France by Weber et al. (2018) allowing to extract OP per mass unit (OP_i) of PM for given source at specific measurement sites. A more recent study of Weber et al. (2021) highlighted biomass burning and traffic emissions as the main OP sources at the national level. While more information is still needed from observations, one of the next steps in the research related to OP_v is to be able to model aerosol OP_v with chemistry transport models (CTM).

Regional CTMs are tools that are already used for operational air quality forecasting in France (Rouil et al., 2009) and in Europe (Marécal et al., 2015). They can also be used for a posteriori epidemiological studies (Adélaïde et al., 2020) and future projections dedicated to support air quality and climate control policies (Cholakian et al., 2021; Fortems-Cheiney et al., 2017). Adding the oxidative potential to the list of simulated species and indicators in these models would be very useful, given its close relation to the ability of aerosols to trigger inflammatory processes and thus its capacity to evaluate health exposure and associated pollution sources (as for example done within the EU Green Deal RI-URBANS project for future Copernicus applications).

The first modelling of the oxidative potential of aerosols was focused on $PM_{2.5}$ over the Eastern US using the DTT test and the CMAQ model (Bates et al., 2018). Using multiple linear regressions with the measured OP by air volume (OP_v) and the source concentrations in the model, the authors were able to obtain the intrinsic oxidative potential (OP_i, OP per mass of PM) of sources. While the results show a higher OP_i for combustion sources, these results were obtained with a relatively limited OP_v dataset available for validation (with a total number of only 187 samples from 4 sites). In Europe, the first OP_v modelling effort used 3 different OP_v tests (among which AA and DTT assays), with a larger number of sites and samples compared to the United States study, and was performed with the CAMx model (Daellenbach et al., 2020). Following a similar approach to the one presented in Weber et al. (2021), an intrinsic OP_i value per source was estimated from a multiple linear regression between OP_v measurements and PM_{10} factor concentrations obtained from PMF studies for the same sites. The PMF factors (mainly organic) were then matched to the simulated sources to represent the oxidative potential of total PM_{10}.

The objectives of this paper are to develop an OP_v modelling tool based on extensive OP_v observations over France, related to source

apportionment studies, and embedded within a chemistry-transport model. The aim is to simulate OP to evaluate its spatial and temporal variability over western Europe with a focus over France, and investigated the contributions of the different sectors of activity. Such an approach is novel for air quality models. With respect to Daellenbach et al. (2020), this work is based on an enhanced observational data set, in terms of variety of sites and chemical composition, allowing to address a larger and more variable set of PM sources (Weber et al., 2018, 2021). In this study, both approaches with a reduced and an extended set of sources will be compared. The CHIMERE-v2020r3 model (Menut et al., 2021) was used, in a specific configuration allowing to quantify PM sources obtained by a Source Apportionment Technology (PSAT) method implemented into the model. Two years (2013–2014) of simulations have been performed to evaluate the model's ability to reproduce the observed PM mass concentrations, the chemical composition and finally the measured PM oxidative potential. The current work focuses on an analysis of sources and variability of the simulated OP_v.

2. Material & methods

2.1. Observations

The years 2013 and 2014 were chosen because of the largest availability of sites where concurrent chemical characterizations, PMF studies, and OP_v measurements are available over France during a period suitable for such modelling work.

2.1.1. PM_{10} concentrations measurements

The PM_{10} concentration datasets are derived from continuous measurements performed by French regional air quality monitoring networks (AQMN). Datasets from a total number of 699 stations are available in metropolitan France for 2013 and 2014. Briefly, two automatic techniques were used at that time by AQMN depending on the site: tapered element oscillating microbalances equipped with filter dynamic measurement systems (TEOM-FDMS, Thermo Scientific), and beta radiation absorption analysers (Met One BAM 1020 and ENVEA MP101M).

2.1.2. Chemical composition

As described by Favez et al. (2021), the French air quality monitoring network is associated with various research projects and programs, converging into a unique operational system for the chemical characterization and subsequent source apportionment of urban aerosols at the national level, known as the CARA program. Additional measurements used in this paper also come from other research programs, like the one conducted at the OPE site (Borlaza et al., 2022).

For datasets used herein, organic and elemental carbon (OC, EC) were measured by thermo-optical analysis using the EUSAAR2 protocol (Cavalli et al., 2010); sugars by liquid chromatography using pulsed amperometric detection (Verlhac et al., 2013; Yttri et al., 2015); measurement protocols are detailed in Samaké et al., 2017, 2019a, b and Weber et al., 2021; the water-soluble inorganic fraction (NO_3^-, SO_4^{2-}, Cl^-, Na^+, NH_4^+, K^+, Mg^{2+}, Ca^{2+}) was measured by ion chromatography (Jaffrezo et al., 2005); Methane sulfonic acid (MSA) as well is measured by ion chromatography (Weber et al., 2021); trace elements (Al, Ag, As, Ba, Be, Br, Bi, Cd, Ce, Co, Cr, Cs, Cu, Fe, La, Li, Mn, Mo, Na, Ni, Pb, Pd, Pt, Rb, Sb, Sc, Se, Sn, Sr, Ti, V, Zn, Zr) were determined by inductively coupled plasma using mass spectrometry or atomic emission spectroscopy (Alleman et al., 2010; Mbengue et al., 2014). These measurement protocols, including OP measurements, have been detailed in previous studies (Calas et al., 2017, Borlaza et al., 2021a, 2021b; Dominutti et al., 2023; Weber et al., 2019).

The present study is benefiting from PM_{10} chemical speciation datasets obtained for 13 different sites and a total number of 2309 daily filter samples. The locations of these sites are illustrated in Fig. 1, while Table 1 provides details on the number of available samples and their temporality.

2.1.3. Source apportionment by a receptor model

Positive Matrix Factorization (PMF) has become the most widely used receptor model for identifying factors contributing to aerosol concentrations (Belis et al., 2020; Grange et al., 2022; Paatero and Tapper, 1994; Waked et al., 2014; Weber et al., 2019). In our work, PMF analyses have been previously conducted using off-line filter-based chemical composition and factor-specific tracers as input data, using a

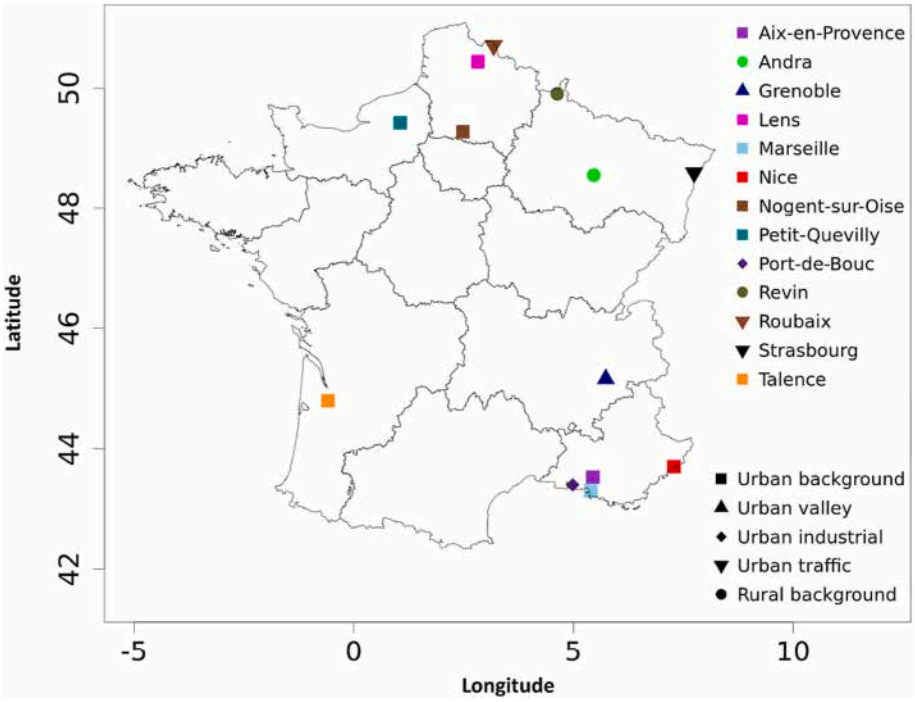

Fig. 1. Location and type of sites used for PM_{10} chemical composition, PMF factor apportionment and oxidative potential measurements from filters over the years 2013 and 2014.

Table 1
Summary of the number of daily filters analysed for PM_{10} composition, PMF factor apportionment and oxidative potential measurements over the years 2013 and 2014 at different French sites. The measurement period and geographical coordinates (latitude; longitude; altitude) are also indicated.

Sites	Coordinates (lat; lon; alt)	Measurement period	Composition	PMF	OP_v
Aix-en-Provence	43.53; 5.44; 192 m	18.07.2013–13.07.2014	117	56	59
Andra-OPE	48.55; 5.46; 386 m	01.01.2013–29.12.2014	98	/	/
Grenoble	45.16; 5.74; 219 m	02.01.2013–29.12.2014	243	240	240
Lens	50.44; 2.83; 47 m	05.04.2013–26.09.2014	158	167	/
Marseille	43.30; 5.39; 73 m	01.06.2014–31.12.2014	95	/	/
Nice	43.70; 7.29; 11 m	04.06.2014–31.12.2014	89	77	62
Nogent-sur-Oise	49.28; 2.48; 28 m	02.01.2013–31.12.2014	220	155	135
Petit-Quevilly (Rouen)	49.43; 1.06; 9 m	01.01.2013–01.06.2014	254	/	/
Port-de-Bouc	43.40; 4.98; 3 m	01.06.2014–31.12.2014	84	80	70
Revin	49.91; 4.63; 394 m	02.01.2013–26.09.2014	192	/	/
Roubaix	50.71; 3.18; 31 m	20.01.2013–08.09.2014	175	/	159
Strasbourg	48.59; 7.74; 139 m	02.04.2013–31.12.2014	108	78	78
Talence (Bordeaux)	44.80; −0.59; 20 m	03.01.2013–31.12.2014	476	38	26

harmonized methodology for each site (Weber et al., 2021). In this study, source apportionment results are obtained for a total number of 891 daily samples collected at 8 sites from early 2013 to end of 2014 (Table 1). Table 2 summarizes the PMF outputs factors along with the main chemical species considered as specific tracers for each of them.

2.1.4. Oxidative potential measurements

On most sites with available source apportionment, measurements of the OP were carried out, after an extraction at iso-concentration to allow sample comparison from different environments. The core protocols include extracting the aerosols from the filters in a simulated lung fluid (Gamble's solution with an additional lung surfactant) at internal body temperature (37.4 °C) without further filtration, a method that allows both the soluble and insoluble parts of the samples to be extracted. To measure the OP via the production of reactive oxygen species (ROS) by PM, these extracts are put in contact with two lung anti-oxidants or surrogates: Ascorbic acid (AA) on the one hand and dithiothreitol (DTT) on the other. ROS production is indirectly measured through AA and DTT depletion over 30 min by spectrophotometry at 265 and 412 nm, respectively. Measurement protocols are described in Calas et al. (2017), Calas et al. (2019), and Dominutti et al. (2023).

The intrinsic oxidative potential (OP_i) per PMF factor was determined by multiple linear regression between the PM_{10} mass concentrations of the factors and the volume oxidative potential (OP_v) (Dinh Ngoc Thuy et al., 2024; Weber et al., 2018, 2019).

Finally, the dataset of OP observations comprises a total of 829 daily measurements obtained from 8 sites for the years 2013 and 2014. Table 1 provides a comprehensive breakdown of these sites used for source attribution, including details such as the time period covered and the number of data points collected at each site.

2.2. Regional modelling

2.2.1. The chemistry transport model WRF-CHIMERE

CHIMERE is a Eulerian state-of-the-art regional chemistry transport model (Menut et al., 2021). It is used operationally by the French platform PREV'AIR and the Copernicus Atmospheric Modelling System (CAMS) (Marécal et al., 2015) to forecast and monitor air quality. The v2020r3 version of CHIMERE coupled with the Weather Research Forecast (WRF, v3.7.1) meteorological model (Skamarock et al., 2008) has been used for this study.

Table 2
PMF factors and associated species used as tracers from Weber et al. (2021).

Factors	Tracers
Biomass burning	Levoglucosan, OC, EC, K, Rb
Primary traffic	OC, EC, Cu, Fe, Sb, Sn
Dust	Al, Ti, Ca
Primary biogenic	Arabitol, mannitol, OC
Aged salt	Na, Mg, SO_4^{2-}, NO_3^-
Nitrate-rich	NO_3^-, NH_4^+
Sulfate-rich	SO_4^{2-}, NH_4^+, Se
MSA rich	Methane Sulfonic Acid (MSA)

For organic aerosol formation and gas/particle partitioning of primary organic aerosol, the volatility basis set (VBS) for the organic species as described in Cholakian et al. (2018) was activated. Resuspension is taken into account by the model only in urban meshes and attributed to primary mineral particles (Loosmore, 2003). The EMEP anthropogenic emission database with a resolution of 10 km^2 provided input data for anthropogenic emissions (Mareckova et al., 2018). Biogenic volatile organic compound (VOC) emissions come from the MEGAN2.1 model (Guenther et al., 2012), NO from soils has been added from EMEP inventories, and biogenic primary organic aerosols are simulated as fungal spores using the Heald and Spracklen scheme (Heald and Spracklen, 2009). The implementation of the latter source into CHIMERE and its evaluation is presented in Vida et al. (2024). Global CAMS reanalysis (Inness et al., 2019) fields are used as initial/boundary conditions with a 3-hourly temporal resolution, providing information on chemical concentrations outside the selected area (Marécal et al., 2015). NCEP-FNL 1° × 1° (NCEP, 2000) resolution global fields are used as boundary/initial conditions for the WRF model.

The simulation has been carried out on a western European domain with a 9 × 9 km^2 horizontal resolution. CHIMERE was run on 9 vertical hybrid levels from ground to an upper height of 500 hPa, the height of the first layer being around 20 m. The model was run in its default 10 bin size configuration for PM size, starting from 0.01 μm and going up to 40 μm in a logarithmic sectional distribution.

As mentioned above, we chose to simulate two complete years, 2013 and 2014, with a temporal resolution 1 h for the outputs. This period was chosen to maximize the number of OP_v observations available while maintaining a reasonable calculation time and having the possibility of carrying out a multi-annual analysis of results.

2.2.2. Sources apportionment and tagging

In our approach, incorporating the PM source information into the model is essential for modelling the OP accurately. The Particulate Source Apportionment Technology (PSAT) developed by Wagstrom et al. (2008) allows to track the contribution of both primary emissions and secondary formation processes for PM concentration. Tagging was preferred to other source tracking methods such as for example brute force simulations because of its cost-effectiveness in terms of calculation time (with only approximately twice the duration of a standard simulation). The sources used for PSAT are the sectors of activity in the Selected Nomenclature for Air Pollution (SNAP) obtained through a correspondence matrix between Nomenclature For Reporting (NFR) and

SNAP. For each species represented in the model, the contribution of different activity sectors present in the emission inventories is obtained (Table 3). The model not only explicitly accounts for natural sources such as mineral dust, marine emissions (Na, Cl, SO_4^{2-}), biogenic emissions (BPOA, BSOA, NO), but also for boundary conditions and for resuspension of primary particulate matter (PPM).

2.3. Description of OP_v modelling methods

To simulate OP_v spatial and temporal variations, we express the volume OP (OP_v in nmol min^{-1} m^{-3}) as the sum, for all the PM sources, of the products of intrinsic OP (OP_i in nmol min^{-1} μg^{-1}) and source mass contribution for each source (μg m^{-3}) (Eq. (1)). OP_v varies as a function of time (t) and the antioxidant/reducer used (a), OP_i varies as a function of the sources considered (s).

$$OP_v^a(t) = \sum_s \left(OP_i^{s,a} * C^s(t)\right) \quad (1)$$

Since the intrinsic oxidative potential OP_i of all individual chemical species contributing to the PM mass is not known, the general idea behind this method is to use the OP_i obtained for the different PM sources composing the PM, as observed from ambient concentrations field studies (Daellenbach et al., 2020; Weber et al., 2021). OP_i values will be combined with simulated source concentrations $C^{t,s}$ obtained by PSAT corresponding in a best possible way to the initial sources (from PMF) used to determine OP_i. Using Eq. (1), we can thus simulate the volumetric OP_v.

2.3.1. OP_v modelling method based on a reduced set of sources

This first method to obtain the source contribution to OP is based on the work of Daellenbach et al. (2020) and is also using Eq. (1). For this method, C^s in the equation is the concentration of PM sources for a specific time (t) derived by PMF. OP_i^s represents the corresponding intrinsic oxidative potential (nmol min^{-1} μg^{-1}), obtained by multiple linear regression between OP_v measurements and PMF factor concentrations C^s, as obtained by Daellenbach et al. (2020). The method is specific for a set of sources restricted to different organic aerosol fractions (see Table 4) that have been obtained from Aerosol Mass Spectrometer (AMS) measurements and PMF analysis at 5 sites in Switzerland, together with OP measurements also performed at IGE (Institut des Géosciences de l'Environnement) according to the same protocols used for our French samples. In addition, the authors added a vehicular-wear source constrained by transition metal filter-based measurements. Based on specific OP measurements from synthetic solutions of reference compounds, the authors made the hypothesis that other aerosol species (especially inorganic salts such as ammonium sulfate and ammonium nitrate) were not contributing significantly to OP_v.

One objective for our work is then to simulate the sources used in Daellenbach et al. (2020) with the CHIMERE model, in order to obtain the terms $C^{t,s}$, and to combine them with their intrinsic OP_i values in Eq. (1) to obtain OP_v. A correspondence table was therefore established between the initial sources in Daellenbach et al. (2020) and their calculation in CHIMERE based on the tagging of EMEP SNAP sectors with the PSAT method. Table 4 displays the correspondence between the PMF factors and the combination of sources tagged in the CHIMERE model as well as the values of the OP_i for AA and DTT assays from Daellenbach et al. (2020). We assume that the "vehicular wear" factor directly corresponds to the simulated primary particulate matter (PPM) associated to the road transport SNAP and the resuspension. HOA (Hydrocarbonlike Organic Aerosol) represents organic aerosols originating from fossil fuel combustion sources. In our simulation, we represent it as a combination of primary organic aerosols (POA) from main combustion sources (SNAP 1, 3, 7 and 8 described in Table 3). BBOA, the biomass burning organic aerosols factor from wood and plant burning is simulated by summing primary organic aerosol concentrations from SNAP 2 and 9 (Table 3). For ASOA (Anthropogenic Secondary Organic Aerosol) and BSOA (Biogenic Secondary Organic Aerosols) factors, we use the secondary organic aerosol concentrations directly simulated by the model which are attributed to explicit model species. ASOA correlates with the oxidation products of aromatic precursors from incomplete combustion and pyrolysis of lignin (Daellenbach et al., 2019).

Table 3
Emission sources in the CHIMERE model.

SNAP	Source name
1	Energy production
2	Residential combustion
3	Industrial combustion (manufacturing)
4	Industrial processes (manufacturing)
5	Extraction & distribution of fossil fuels
6	Solvents
7	Road transport
8	Other transports
9	Waste treatment
10	Agriculture
/	Resuspension
/	Boundary conditions
/	Mineral dust
/	Marine
/	Biogenic

Table 4
Correspondence between PMF factors and CHIMERE sources for the reduced set method and their intrinsic oxidative potential (OP_i) for DDT and AA tests with median interquartile range in nmol min^{-1} μg^{-1} in Daellenbach et al. (2020). SNAP numbers are indicated with "S number".

PMF factors Daellenbach et al. (2020)	PSAT CHIMERE	OP_i^{DTT}	OP_i^{AA}
Vehicular wear	PPM road transport (S7) + resuspension	**3.51** [3.29–3.76]	**3.16** [2.56–3.38]
HOA	POA energy production (S1) + industrial combustion (S3) + road transport (S7) + other transports (S8)	**0.94** [0.79–1.10]	**0.00** [0.–0.]
BBOA	POA residential combustion (S2) + waste treatment (S9)	**0.08** [0.01–0.14]	**0.06** [0.03–0.23]
ASOA	ASOA all anthropogenic sources (S1 to S10)	**0.44** [0.35–0.43]	**0.42** [0.36–0.48]
BSOA	BSOA	**0.15** [0.11–0.20]	**0.00** [0.–0.]

2.3.2. OP_v modelling method with an extended set of sources

In addition to the first approach described in Section 2.3.1, a new method has been established and tested, directly based on the work of Weber et al. (2021). This second method enables the consideration of an extended set of aerosol sources when modelling the OP, as opposed to the reduced set of the first method. In this approach, intrinsic OP_i is again obtained from multi-linear regression between observed OP_v and aerosol sources obtained by PMF, but this time from 15 sites in France. In this study by Weber et al. (2021), the authors were careful to check, as much as possible, that the factors chosen were common to the different sites. This homogeneity of factors means that they can be extrapolated to the whole of France with greater confidence. The PMF results were not restricted to particular sources like in the reduced set approach for which factors associated to inorganic species were excluded.

In order to calculate OP_i from Eq. (1), the challenge lies again in establishing a correspondence between the observation-based sources resulting from the PMF factors and the simulation-based sources derived from PSAT analysis (see Section 2.2.2), but in this case for an extended list of sources corresponding less directly to modelled species compared to the first approach (but much more to the phenomenology of the field measurements). The approach adopted to resolve this issue is explained

hereafter first in a general way and then source by source.

At first glance, and from common geophysical expertise, some sources can be easily reconciled like the PMF biomass combustion factor with the PSAT residential combustion source, for which the majority of carbonaceous aerosol stem from wood burning. For aged salt, secondary species from the "other transports" sector were included, because they are often located on water surfaces. The traffic emissions from road transport are identified from both PMF and PSAT as a mainly primary source. Other PMF factors are more difficult to associate directly to one specific SNAP such as nitrate-rich, sulfate-rich, or MSA-rich and it is not obvious how to directly reconcile them with emission sectors used within the CHIMERE model. For all these sources, several tests between PMF factors and combinations of PSAT sources were conducted to finally propose the matches shown in Table 5 and described in more details below. To achieve this, we performed here a comparison between the observed source chemical profiles and the model-generated profiles. Additionally, we combined specific PSAT sources and compared their temporal patterns with those obtained through PMF factors. This comparison allows for a comprehensive evaluation of the similarities and differences in the temporal behaviour of the identified sources. Eventually, the final choice was validated through a statistical analysis (correlations, biases, errors).

2.3.2.1. Biomass burning. The chemical profile of the biomass combustion factor from PMF is mainly composed of organic matter with a median value of about 95 % over all sites, with very few elemental carbon and secondary inorganic aerosols contributing to this source (Fig. 2). In the PMF method, levoglucosan is a tracer for primary organic aerosol from this factor, but secondary organic aerosol formation from this source is probably included as well as long as it remains correlated with levoglucosan. It was therefore decided to create an equivalence in the model with the SNAP 2 residential combustion source, and to include both the primary and the secondary fractions. Fig. 2 illustrates the major contribution of OM to the PSAT SNAP 2 source (>50 %), as for the PMF outputs. However, there is also a significant fraction of NO_3^- in PSAT due to NO_x emissions from various combustion sources in the residential sector; this could not be distinguished from wood burning in the available emission data. A specific SO_2 source from oil fuel use was excluded and attributed to sulfate-rich PMF factor.

Table 5
Correspondence between PMF factors and CHIMERE sources for the extended set method. For some sources, only primary (PRIM) or secondary (SEC) species have been taken into account. SNAP numbers are indicated with "S number". The two last columns indicate the intrinsic OP values for both DTT and AA assays in nmol min^{-1} μg^{-1} from Weber et al., 2021. Within the table PRIM stand for primary and SEC for secondary.

PMF factors Weber et al., 2021	PSAT CHIMERE	OP_i^{DTT}	OP_i^{AA}
Biomass burning	Residential combustion (S2) without SO_4	0.13 [0.10–0.18]	0.17 [0.13–0.26]
Primary traffic	Road transport (S7) without NO_3	0.21 [0.17–0.27]	0.14 [0.07–0.23]
Dust	PRIM industries (S1 + S3 + S4 + S5+ S6 + S9) + Agriculture (S10) + Mineral dust + Resuspension	0.11 [0.08–0.15]	0.01 [0.00–0.04]
Primary biogenic	PRIM Biogenic + Other transports (S8)	0.13 [0.05–0.18]	0.02 [0.00–0.04]
Aged salt	Boundary conditions + Marine + SEC Other transports (S8)	0.04 [0.03–0.12]	0.02 [0.00–0.05]
Nitrate-rich	SEC Agriculture (50 % S10) + SO_4 (Residential, S2) + NO_3 (Road transport, S7)	0.04 [0.03–0.18]	0.01 [0.01–0.03]
Sulfate-rich	SEC Industries (S1 + S3 + S4 + S5 + S6 + S9) + Agriculture (50 % S10) + Biogenic	0.09 [0.04–0.12]	0.01 [0.01–0.02]
MSA rich	Not modelled	0.12 [0.02–0.29]	0.00 [0.03–0.07]

2.3.2.2. Primary traffic. The corresponding PMF chemical profile (Fig. 2) indicates an EC contribution to this source of about 20 %. Metals, some of which -such as Cu - being commonly considered as tracers of road traffic emissions, contribute to about 10 % (grouped into PPM - inorganic primary particulate matter). Fig. 2 shows that, as for biomass burning, OM is the major fraction (~55 %), and can be both primary and secondary, as long as secondary OM from this source is correlated with the specific primary tracers. Therefore, the road transport source (SNAP 7) was used, excluding nitrates from traffic related NO_x emissions which were affected to the nitrate-rich PMF factor. In this way, the modelled chemical profile is similar to the observed one; OM being the major species followed by EC and PPM.

2.3.2.3. Aged salt. This factor concerns mainly aerosols with a marine origin including sodium, magnesium, chloride, as specific tracers in the PMF (Fig. S1). The chemical profile of this source shows a major contribution of sodium and chloride, but also shows a contribution of nitrate (about 15 %) pointing to ageing of sea-salt (replacement of chloride by nitrate). The sulfate contribution (~10 %) could be due to secondary aerosols from ship emissions together with sea-salt-sulfate. The PSAT modelling of this source therefore takes into account the entire marine salt source as well as the SNAP 8 including sources of emissions linked to transport other than road traffic. It also includes PM from the boundary conditions, because they are often advected by westerlies from the Atlantic Ocean, and could therefore be included with the marine "aged salt" source. In the PSAT source profiles, Na^+ and Cl^- are still important contributors (respectively ~15 % and 20 %) albeit lower than in PMF, while NO_3^- makes up about 30 % indicating the secondary character of aged sea-salt.

2.3.2.4. Nitrate-rich. The nitrate-rich factor is a secondary aerosol source consisting of a large fraction of ammonium nitrate as well as gathering some fractions of other secondary aerosol species. As nitrate is derived from NO_x emissions in fossil fuel combustion processes, especially from transport, the link with the road transport source in the model is direct. Ammonium is considered as mainly originating from agricultural activities and the associated ammonia emissions, so the agricultural source of the PSAT has been used to simulate the Nitrate rich factor of the PMF, but only partially (50 %), as both nitrate and ammonium sulfate are secondary (Fig. S1). Both PMF and PSAT chemical profiles are in rather good agreement, NH_4^+ and NO_3^- being the major contributors (~ 65 % in PMF, ~85 % in PSAT). In the PMF, OM contributes to nearly 20 %. This is probably secondary organic aerosol formed at a time scale of about a day compatible with that of nitrate formation. In our PSAT approach, this SOA is attributed to the corresponding primary sources, and especially BSOA is attributed to the sulfate rich source. Minor contributions are also coming from sulfate (~15 % in PMF, ~10 % in PSAT).

2.3.2.5. Sulfate-rich. The sulfate-rich factor is a secondary aerosol source including a large fraction of ammonium sulfate or bisulfate, also including other secondary aerosol species (Fig. S1). It is probably representative of more aged secondary aerosol, as the conversion of SO_2 into SO_4^{2-} in the gas phase takes several days or requires the presence of cloud water. It contains a specific metallic tracer, selenium, that may arise from industrial activities such as glass, cement, fertilizer or metallurgy production, but also from natural sources. The presence of secondary organic matter in this factor comes mainly from biogenic secondary organic aerosols (BSOA), as identified with a specific α-pinene tracer, the 3-MBTCA, in a study performed on some of the same sites as ours (Borlaza et al., 2021a, 2021b). In the PSAT approach, BSOA has been attributed to this factor. Furthermore, concentrations of sulfate and oxalate (the most important organic acid by mass, indicative of aged

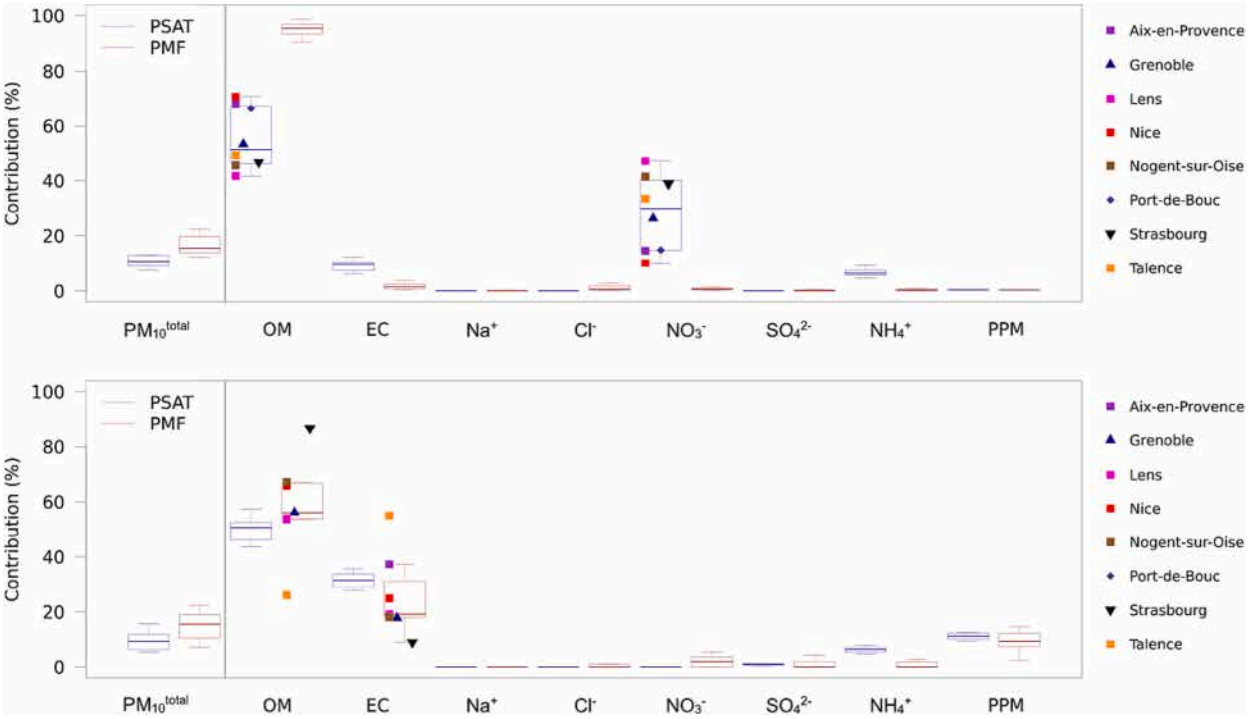

Fig. 2. Comparison of chemical profiles of biomass combustion sources (top) and primary traffic (bottom) from MFP (red) and CHIMERE simulation with PSAT (blue). Model mean values are calculated over 2013 and 2014. The ordinate represents the relative contribution of the species included in the source. The PM10 column shows the source's contribution to PM10. Values for individual sites are shown only where variability is significant. For other sources, the figures can be found in the supplement (Figs. S1 and S2).

organic matter) are always well correlated in many studies. Both PMF and PSAT chemical profiles are rather similar, the sum of SO_4^{2-} and NH_4^+ accounting for respectively ~45 and ~40 % and OM for respectively ~45 and ~50 % for each case.

2.3.2.6. Dust. In the PMF analysis, this factor contains metal-rich particles with aluminium, titanium and calcium as tracers. However, the major contributor is actually OM, with a smaller fraction of EC (Fig. S2). This could be due to the difficulty of the PMF analysis to fully resolve different sources, or to the fact that road dust resuspension is also strongly contributing to this PMF factor, with all the sites where this factor appears being urban ones. The chemical composition of resuspended road dust is not fully elucidated (Rienda and Alves, 2021) and probably not totally homogeneous spatially, but it can be expected that it contains organic aerosol and EC from anthropogenic sources (Charron et al., 2019), as urban aerosol generally does. In addition, important fractions of plant debris have been found in resuspended aerosol (Brighty et al., 2022). We then have simulated the PMF dust factor as mineral dust, resuspension as well as adding the primary mineral emissions from industrial and agriculture sectors (Table 5). However, as the chemical composition of resuspended aerosol is not fully known, it is uniquely affected to the PPM species in CHIMERE, even if it certainly contains a large fraction of carbonaceous aerosol. This partly explains the missing OM fraction in the PSAT chemical profile.

2.3.2.7. Primary biogenic. The primary biogenic factor is composed of biogenic organic aerosols directly from vegetation. Polyols are used as tracers of this primary biogenic organic matter, which is mainly emitted from fungal spores in the PM_{10} fraction (Samaké et al., 2019a, 2019b). Thus, OM is the major contributor (about 90 %) to this chemical profile, with a small contribution from EC (around 5 %) that could partly be associated with agricultural machinery (Fig. S2) or some soil dust resuspension. With PSAT, we combined both primary biogenic organic aerosol emissions and primary emissions from other transport. This results in a major OM contribution (about 80 %) and a minor EC contribution (~10 %).

2.3.2.8. MSA-rich. This PMF factor is composed exclusively of biogenic secondary species linked to the biological activities of marine and (possibly) lacustrine plankton or algae. It should be noted that marine aerosol or precursor sources have not been included in the CHIMERE simulation, except the gaseous DMS (Dimethyl Sulfide). As this PMF factor is only available at some of the sites and it is always a minor of PM mass (<5 % PM_{10}), omitting this factor will only have a very limited effect on the modelling of the oxidative potential of aerosols.

In conclusion, the major chemical contributors to pairs of PMF factors and PSAT sources are in general at least in qualitative agreement but for the case of dust for which the fraction in PM_{10} is similar between PMF and PSAT combination of sources but the contribution of different species if significantly different. Overall, these correspondences allow the use of intrinsic oxidative potential values obtained for PMF factors to the corresponding PSAT sources. However, this procedure still bears some uncertainty; nonetheless this uncertainty seems acceptable in light of other existing uncertainties (e.g. the uncertainty to quantitatively model the different PMF factors (evaluated in Section 3.2), or the uncertainty in the OP_i values themselves, derived as the median of a limited number of sites (Weber et al., 2021)).

In addition to the median OP_i values per source, we have indicated, for the DTT and AA tests, the interquartile ranges of these values obtained by Daellenbach et al. (2020) (Table 4) and Weber et al. (2021) (Table 5), which reflect the inter-site variability of these values. This gives an idea of the robustness of the median values we use. We can see that for the sources with the highest OP values for the two tests, primary traffic and biomass burning, the interquartile variability is not too high compared to the median. However, for the DTT test, the primary biogenic and especially the MSA-rich sources show greater variability, which raises questions about the representativeness of the median values chosen.

3. Evaluation of the simulation with observations

In this section, we evaluate and analyze the ability of the CHIMERE model to reproduce daily observed PM_{10} concentrations, PM composition, PMF factors and OP_v measurements. For this performance evaluation of the model, from a technical point of view, we compared the simulated daily mean values to the observations since this is what was available for the OP_v. The simulated PM_{10} and species concentrations at the sites are obtained by bilinear interpolation of the results from the 4 grid cells adjacent to the site in the model.

3.1. Particulate matter

3.1.1. PM_{10} concentrations

Fig. 3a and b displays the maps of the correlation coefficients (Pearson R) calculated for PM_{10} mass for the whole simulation period (2013–2014) and all days (when available) on all PM_{10} stations in France. It shows the overall ability of the CHIMERE model to reproduce variations of daily PM_{10} concentrations. Indeed, we get correlations higher than 0.60 for most sites. This is quite satisfactory compared to the CAMS ensemble (Marécal et al., 2015). However, simulations for sites in mountainous areas (e.g., alpine region) exhibit lower correlations. This is partly explained by the fact that the model resolution of 9×9 km^2 does not resolve orography and related dynamical processes, such as thermal winds and inversion layers (Bessagnet et al., 2020).

Concerning the mean fractional bias (MFB) visible on Fig. 3 for the same period, the average on all sites is 2.61 % for 2013 and 4.08 % for 2014 which is low. For the majority of the sites, the bias is in a range of ±30 % which can be considered as satisfactory according to the recommendations of Boylan and Russell (2006). On the other hand, there is a North/South disparity, with overestimations that can be important for the sites in the North East of France and underestimations in the South East. Fig. 3 shows that the results are very similar from one year (2013) to another (2014). The RMSE maps (Fig. S3) show an error structure similar to that shown for the biases (Fig. 3).

The type of site (urban, suburban, rural) does not seem to impact the simulation of daily average PM_{10} concentrations that much as opposed to the geographical situation (e.g., mountainous regions vs. flat lands and north vs. south location).

3.1.2. Chemical composition of PM_{10}

Since we are interested in a health impact indicator that integrates both the chemical composition of particles and OP_i by PM source, it is important to assess how well the model reproduces this chemical composition. We carried out a rather complete comparison of the simulations and daily observations available for the French sites over the period of the study. Nevertheless, in the framework of this paper, we do not have the objective to go too deep in the analysis of model's capabilities but rather to be able to further analyze the potential weaknesses in the OP_v modelling.

From observations at the sites mentioned in Section 2.1.2, the following species concentrations have been used in the analysis: Organic carbon (OC), elemental carbon (EC), nitrate (NO_3^-), sulfate (SO_4^{2-}), ammonium (NH_4^+), sodium (Na^+) calcium (Ca^{2+}) and "dust". For the comparisons with simulated concentrations, we had to propose some conversions to fit the measured species with the simulated ones. Measured OC were multiplied by a factor 1.80 to obtain the organic matter (OM) concentrations (Favez et al., 2010; Petit et al., 2015). To

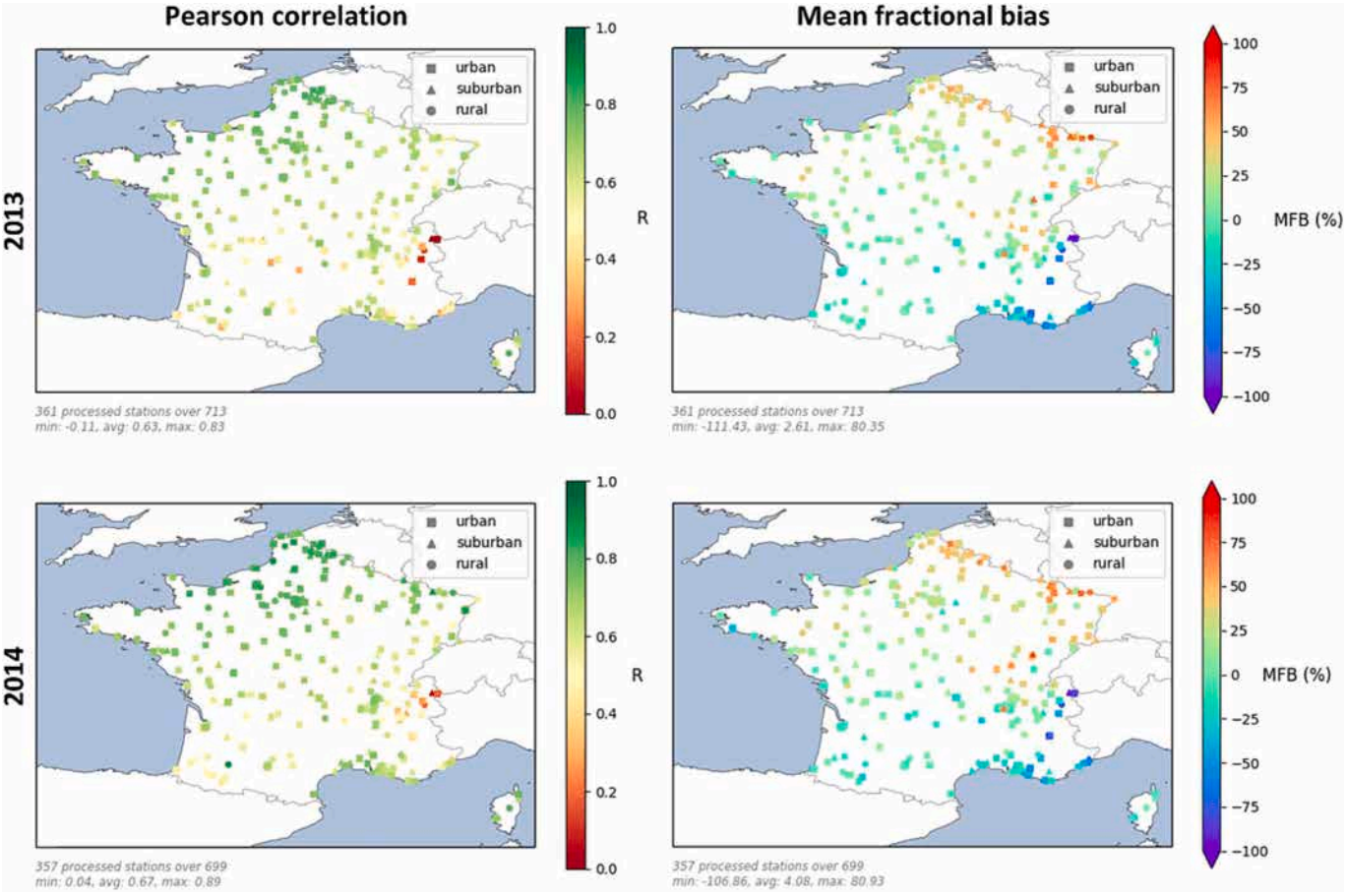

Fig. 3. Scores between PM_{10} daily mean mass concentrations measured and modelled by CHIMERE. Pearson correlation (R) is visible on the left from bottom to top respectively for 2013 and 2014. The same goes for mean fractional bias (MFB) on the right.

obtain dust concentrations, a factor of 8 was applied to measured Ca^{2+} concentrations (Favez et al., 2008).

Fig. 4 shows that for these latter two PM components, the correlation values between simulation and observations are lower than for the other components with a median of about 0.35 for OM and about 0.30 for dust. In addition, there is a very large disparity in scores depending on the site, with R ~ 0 for Aix-en-Provence, Nice or Roubaix, and R ~ 0.58 for Lens and Revin in the case of OM. Correlations are in the same ranges for dust. We note much better performances for reproducing EC and SO_4^{2-}, with median values for R respectively of 0.58 and 0.59, and more homogeneous behaviour for different sites. For NO_3^-, NH_4^+ and Na^+ the scores are even better with respective median R values of 0.60, 0.62 and 0.60. These scores are in a good agreement, for the inorganic fraction, with those presented in Couvidat et al. (2018). Overall, these comparisons indicate that there are certain difficulties in reproducing OM and dust for which sources are apparently not yet well reproduced by the model according to the sites. For organic matter, we can see that the main difficulties seem to be associated with sites in the south of France (Nice, Aix, Port-de-Bouc) and mid latitude (Talence and Grenoble), which may reflect the difficulty in simulating some sources or some transport / dynamic processes in the atmosphere of these areas. In addition, a single OM/OC conversion factor may not reflect the variability in this ratio, lower for primary and higher for aged secondary aerosol. We can note that this is also consistent with the fact that it is more difficult for the model to reproduce PM_{10} concentrations in the southeastern part of France, where OM represents a larger fraction of the PM_{10} (Font et al., 2024).

We also note that the chemistry at some specific sites is more difficult to reproduce by the model. This is particularly the case for the Roubaix traffic site, which is perhaps influenced by sources that are too local for the current model spatial resolution, even if conversely, the chemistry at the Strasbourg traffic site is very well simulated. There also seems to be some difficulty in reproducing the PM chemistry at the ANDRA-OPE site; it is however a remote rural site and therefore it should not suffer from problems of representativeness which can penalize sites near point sources, or valley sites such as Grenoble where sources and dynamics are difficult to represent at the scale of 9 × 9 km^2. In the following discussion concerning modelling of OP_v, it will be necessary to be cautious in the interpretation of the simulated values, particularly depending upon the sites considered.

The bias analysis (here the mean fractional bias) is also considered and provides another aspect to take into account. Biases are in general reasonable (in the sense of the criteria by Boylan and Russell (2006)), with values largely between ±50 % for OM, EC, SO_4^{2-} and dust. Conversely, there is a strong tendency of the model to overestimate NO_3^- and NH_4^+ concentrations (i.e. ammonium nitrate), particularly for the sites in the North of France with bias values between 50 and 100 %. This is consistent with the strong biases observed on the simulation of PM_{10} concentrations in the North East of France, where nitrate is a major PM_{10} component. This type of bias has also been observed at European level by Couvidat et al. (2018), albeit in lower proportions. A hypothesis may be considered that the issue comes from biases in the representation of ammonia emissions of the agricultural origin or in the inorganic chemistry associated with the formation of nitric acid and then the neutralization of this acid by ammonia. This is also suggested in the comparisons between NH_3 emission inventories and IASI satellite observations (Fortems-Cheiney et al., 2020). Note also that there is no specific bias in the representation of NO_2 emissions and its concentrations compared to NO_2 measurements on French sites (not shown). We also must note that negative sampling artefacts are also possible (Schaap et al., 2004), potentially leading to significant underestimations of ammonium nitrate from filter-based analysis. To complete the analysis, RMSEs are displayed in Fig. S4 and show that species with higher biases (but good correlations) such as nitrate and ammonium have the highest errors, as do species with lower biases but poorer correlations such as OM and dust. Moreover, it is interesting to see that there is a greater dispersion for nitrate in terms of RMSE.

3.2. Source modelling

As extensively underlined in Section 2.3.2, one of the key points of the OP simulation methods is the simulation of the PMF factors from the PSAT sources of the model. For the so-called extended method which takes into account all the factors of the PMF, we have established a

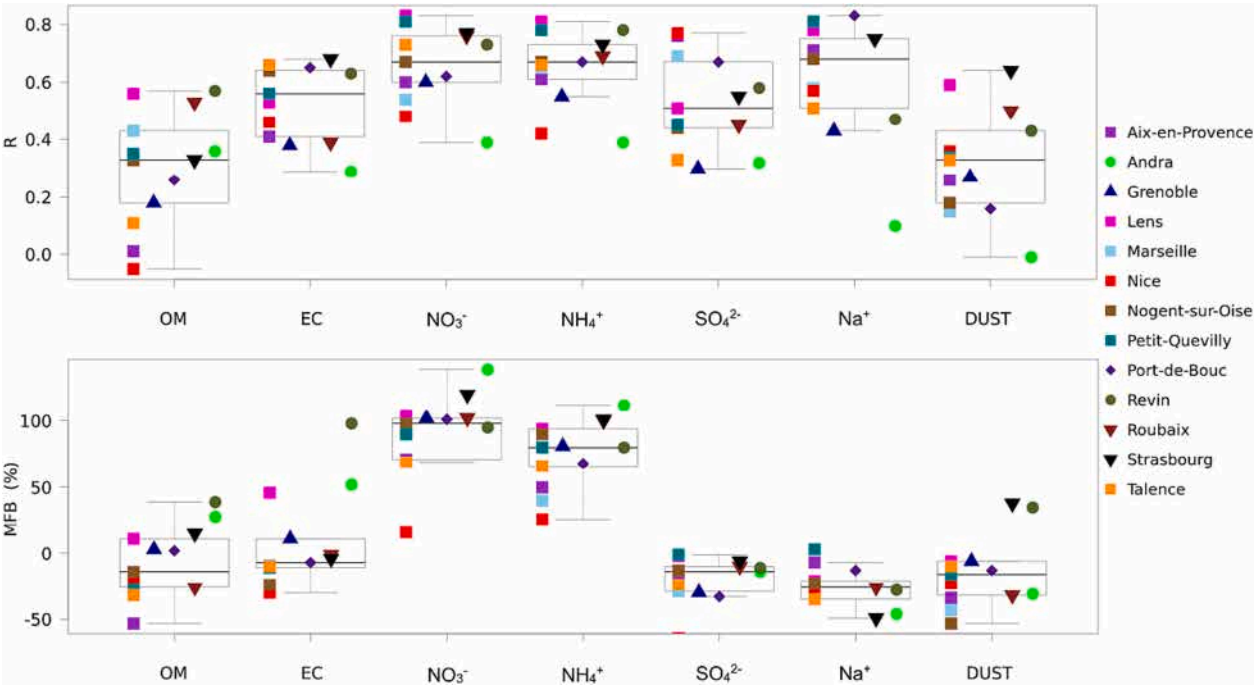

Fig. 4. Statistical scores of the chemical composition of PM_{10} between daily mean concentrations measured and those modelled by CHIMERE. Pearson correlation (R) on the top graph and mean fractional bias (MFB) on the bottom one for 2013 and 2014.

correspondence between PMF factors, PSAT sources and model species (Table 5) and compared their chemical profiles (Fig. 2). Here, we perform a statistical analysis (Fig. 5) (correlations and biases) of daily time series from the PMF factors and their simulation by CHIMERE with the correspondences proposed in Table 5.

The median correlations of the daily mean source specific concentrations at all sites are in the range of 0.30 to 0.70. Correlation is on the lower end for the dust factor, which is consistent with the model's difficulties in simulating soluble calcium (Section 3.1.2). The high variability, particularly the low and even negative correlations at Aix-en-Provence and Port-de-Bouc, could be partially explained by the identification of an industrial PMF factor, which was not taken into account in the final harmonized PMF because it was identified at only two sites; for these two sites, this factor was then integrated into the dust factor. For Strasbourg, the difficulty lies probably in modelling the resuspension of aerosols at a traffic site. The PSAT and PMF factors of aged salt correlate at around 0.40 on average, being not well simulated at 3 sites (Lens, Nogent-sur-Oise and Strasbourg) all located in the northern eastern part of France. The opposite is seen for the primary biogenic PMF factor, with clear difficulties for the sites of the Mediterranean coast (Aix-en-Provence, Nice, Port-de-Bouc). As for the other factors (Biomass burning, Nitrate-rich, Primary traffic and Sulfate-rich), the median correlations are >0.40 with less variability among sites than for the sources previously mentioned, reflecting a certain homogeneity in the results.

As far as biases are concerned, the differences are particularly marked for very local and mainly primary sources such as primary traffic and biomass burning. Conversely, secondary inorganic sources such as nitrates are generally overestimated; this feature is also observed on RMSE (Fig. S4). Such results are commonly observed in regional models, where accurate representation of source contributions from localized influences at specific sites remains challenging (Marécal et al., 2015). As mentioned above, underestimations from filter-based measurements due to negative sampling artefacts of semi-volatile species, such as ammonium nitrate, cannot not be excluded either. The site typology does not seem to affect the results. In addition, some PMF factors observed at specific sites only were not considered in our work as our approach needs to be general for France. This could lead to biases, as these sources in return are affected by other sources that are represented in our PSAT approach, and then not taken into account in the PMF approach. Nevertheless, the (MFB) biases are fairly low for all the sources, within ±50 %, except sulfate-rich with a positive bias of +65 %.

Finally, PMF and simulated concentrations for the primary biogenic source show a median correlation of about 0.30 and a median MFB of about −20 %. The modelling of primary biogenic aerosols, in particular the organic fraction, by simulating fungal spores is discussed in detail in a separate paper (Vida et al., 2024).

For the method using a reduced set of sources, this correspondence is based on the one carried out in another regional transport chemistry model (CAMx) as part of the modelling of the oxidative potential of aerosols in Switzerland and Europe (Daellenbach et al., 2020). No comparisons of the time series were made due to the complexity of accessing the data. However, the source contribution maps for PM_{10} and oxidative potential are similar between the original work of Daellenbach et al. (2020) and our application.

3.3. Oxidative potential modelling

The last stage of the evaluation of the model performance concerns the simulation of the OP_v itself. We simulated the volume OP_v for the two complementary tests, AA and DTT, as described in Section 2.3. We then compared these simulated OP_v values to the daily values observed at different sites, for the two methods developed, i.e. the "reduced set" method and the "extended set" method. The overall results are presented in Fig. 6 which show the correlations and the biases between simulations and observations and Fig. S4 for the RMSE.

The medians of daily correlation values are around 0.35 and 0.50 for the reduced source set method for AA and DTT respectively. Median correlations are better for the method using a larger number of sources, approximately 0.50 for AA and 0.60 for DTT. Time series are hardly reproduced at Aix-en-Provence, where the correlations are systematically below 0.20 for AA and DTT, whatever the method (Figs. S3 and S5). The same applies to the Nice site, but with slightly better correlations for DTT. We also note that the correlation for the Grenoble site is lower than the general median in all cases. For all these sites, the results

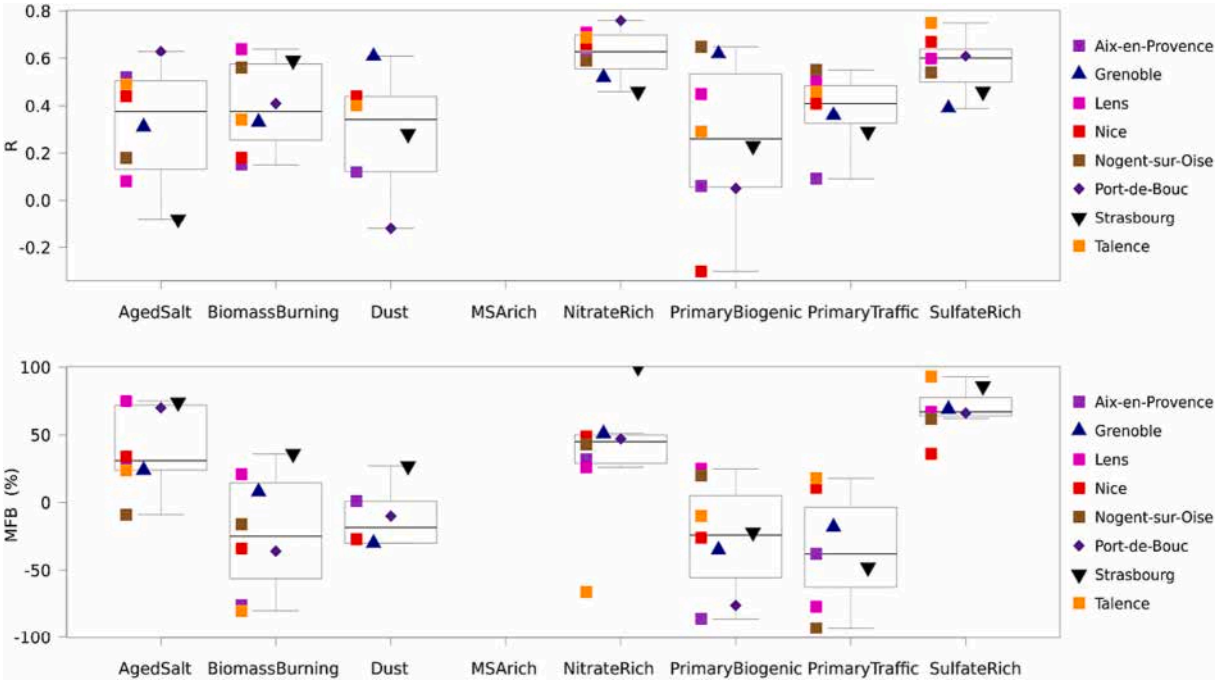

Fig. 5. Statistical scores of the modelled sources between daily mean concentrations of sources from PMF extended set method and those modelled by CHIMERE. Pearson correlation (R) on the top and mean fractional bias (MFB) on the bottom for 2013 and 2014.

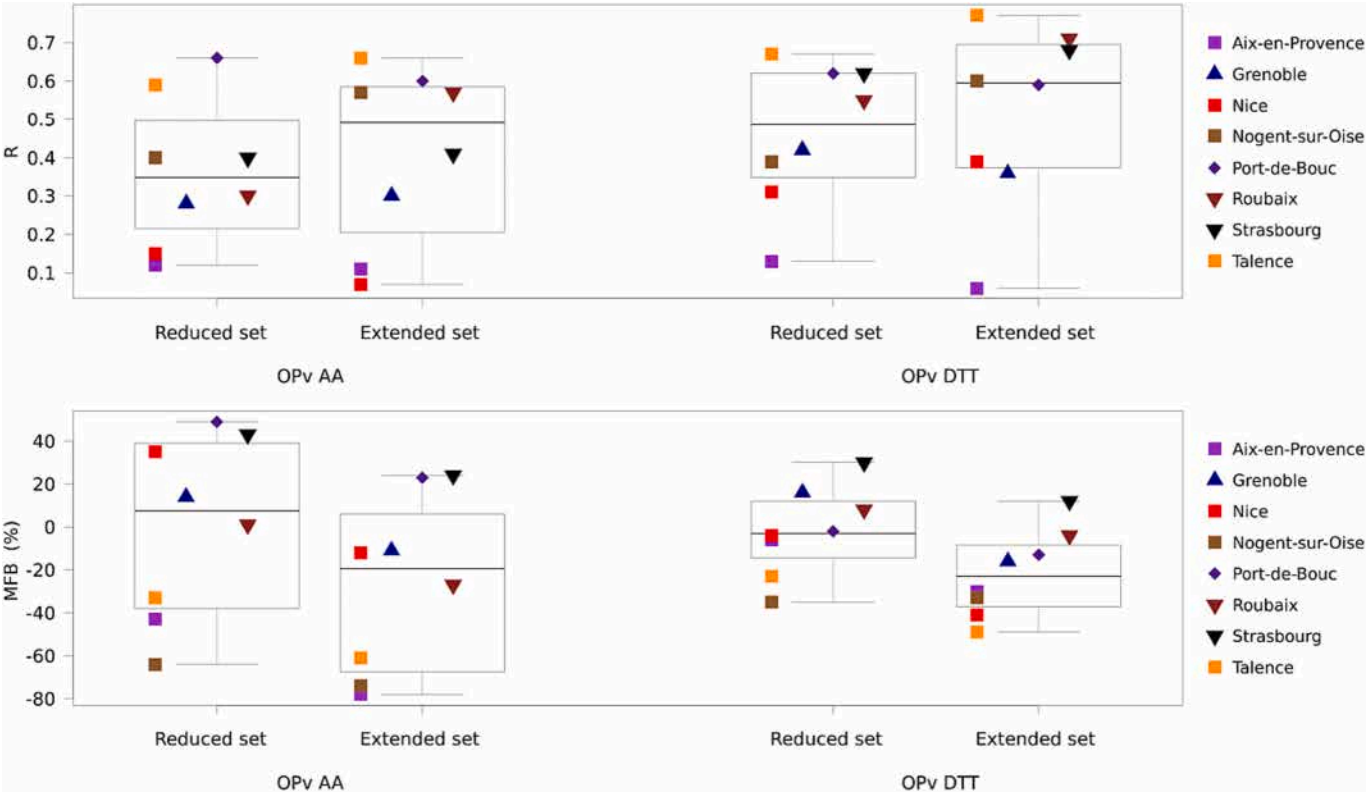

Fig. 6. Statistical scores of the modelled oxidative potential between daily mean measurements and those modelled by CHIMERE. Pearson correlation (R) on the top and mean fractional bias (MFB) on the bottom for 2013 and 2014. Station time series for AA are available in the supplement (Figs. S5 and S6), as are those for DTT (Figs. S7 and S8).

align with the low correlations in simulating the composition of PM sources and especially OM. Conversely, for sites with less complex orography, correlations are in general much better, as for Talence, with correlation about 0.60 and 0.70 for the reduced set of sources and about 0.70 and 0.80 for the extended set, respectively for the AA and the DTT assays.

Median biases in simulated OP_v are in general small, between about zero and − 30 % for MFB. Particularly, for the reduced set MFB values are about zero for AA and about −10 % for DTT. For the extended set the corresponding values are a bit larger at about −30 %, both for AA and DTT, albeit with large regional differences. These small biases are an important result of this study given the various uncertainty factors contributing to simulated OP_v. Negative biases can often be related to underestimations of primary sources of PM_{10} from biomass combustion and primary traffic. These sources both have a very high intrinsic OP_i, this may explain the underestimation of the OP_v for the extended set method. As for PM_{10}, biases are highly variable for different sites.

An important difference can be observed between the results obtained with the two OP assays (Fig. 6). For the AA test, it is striking to see the significant bias at the Nogent-sur-Oise site (MFB around −80 %). It is likely explained by the very low contribution of the primary traffic source at this site in the simulations, a source with one of the highest OP_i. For Nogent again, but also for Talence and Aix-en-Provence, the important negative bias of the biomass burning source can also explain the important biases observed for OP_v^{DTT} (Fig. 6). It should be noted that RMSE (Fig. S4) exhibit very similar feature than bias in terms of ranking of the two methods and tests.

In addition, to support this analysis, we have plotted station time series for AA (Figs. S5 and S6) and for DTT (Figs. S7 and S8). Each time skill scores (MFB, R and RMSE are indicated.

As a conclusion, in comparing the reduced and the extended set methods, we can note a better correlation for the latter one, and acceptable bias for both methods. In addition, the extended method has a broader acceptance of all kinds of sources and not excluding them a priori.

Although this study is based on a large number of OP data compared with what exists in the literature, it should be noted that the number of OP data available per station is sometimes low and does not allow a complete assessment of seasonal cycles. The number of data by type of site is sometimes unbalanced, with a lot of data for alpine sites, which limit a bit the conclusions on the performance of the methods developed. This calls for further studies based on larger volumes of data. To improve the method's representativeness, more OP and intrinsic OP data from more sources will be needed in the future, and harmonized if possible.

4. OP spatial distribution over France

4.1. *Spatialization of OP_v*

Here we present 2D maps of simulated OP_v over France as an annual average for 2013 and 2014 (Fig. 7). Globally, they show, as expected, higher oxidative burden exposure related to aerosols in large agglomerations and densely populated areas leading to higher exposure for the urban French population. Also, major roads such as motorways are prominently identifiable in the spatial distribution of OP_v. However, there are differences depending on the test used (DTT or AA) and the method used (reduced or extended set).

When the same method is used (e.g. reduced or extended set), we can see that OP_v^{AA} and OP_v^{DTT} show similar patterns overall, but with differences in the intensity of certain sources and in spatial gradients. This can be attributed to differences in OP_i between the same PMF factors for both tests. We know that OP_i values are relatively larger for the AA than for the DTT assay (Tables 4 and 5) for mainly primary sources (primary traffic, primary biomass burning) as compared to secondary sources

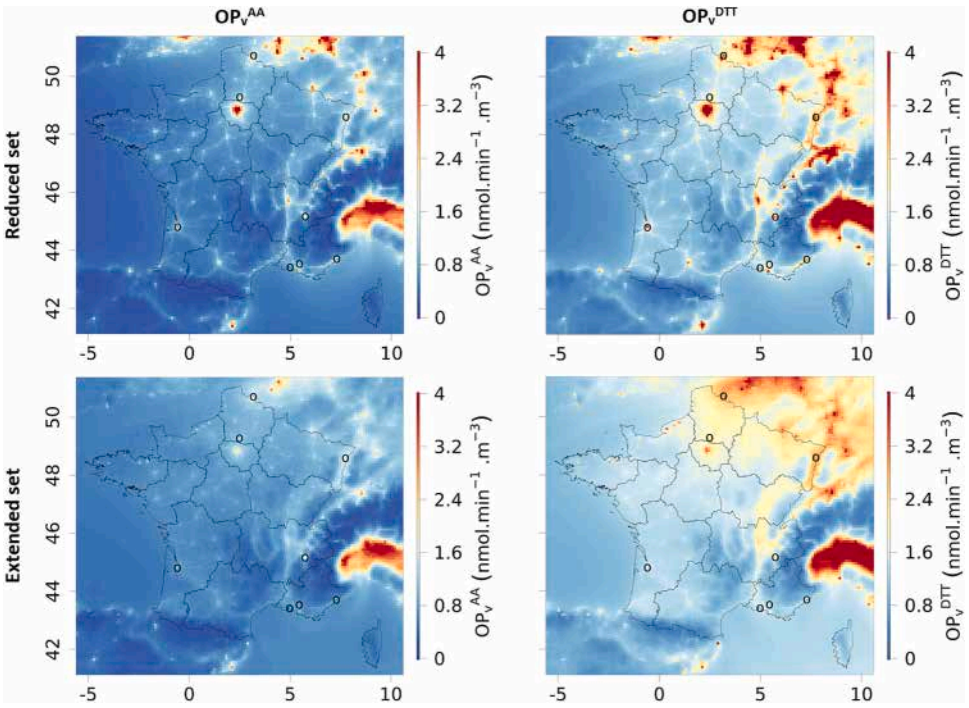

Fig. 7. Volume oxidative potential (OP_v) modelled with the reduced set method on the top and extended set on the bottom depending on the OP assay, OP_v^{AA} on the left and OP_v^{DTT} on the right. Biannual mean oxidative potential (2013–2014) in the first layer of the CHIMERE model. The black circles represent the OP_v measurement sites in France.

(nitrate-rich, sulfate-rich). This leads to relatively higher values of OP_v^{AA} over larger and more urbanized areas compared to OP_v^{DTT}.

In addition, OP_v intensities differ between the two simulation methods using a reduced ($OP_v^{AA,red}$, $OP_v^{DTT,red}$) or extended ($OP_v^{AA,ext}$, $OP_v^{DTT,ext}$) set of sources. Indeed, the background intensity is higher when using the extended set due to taking into account inorganic species in the analysis by including OP_i values for factors such as nitrate-rich and sulfate-rich. On the contrary, OP_v values for urban agglomerations

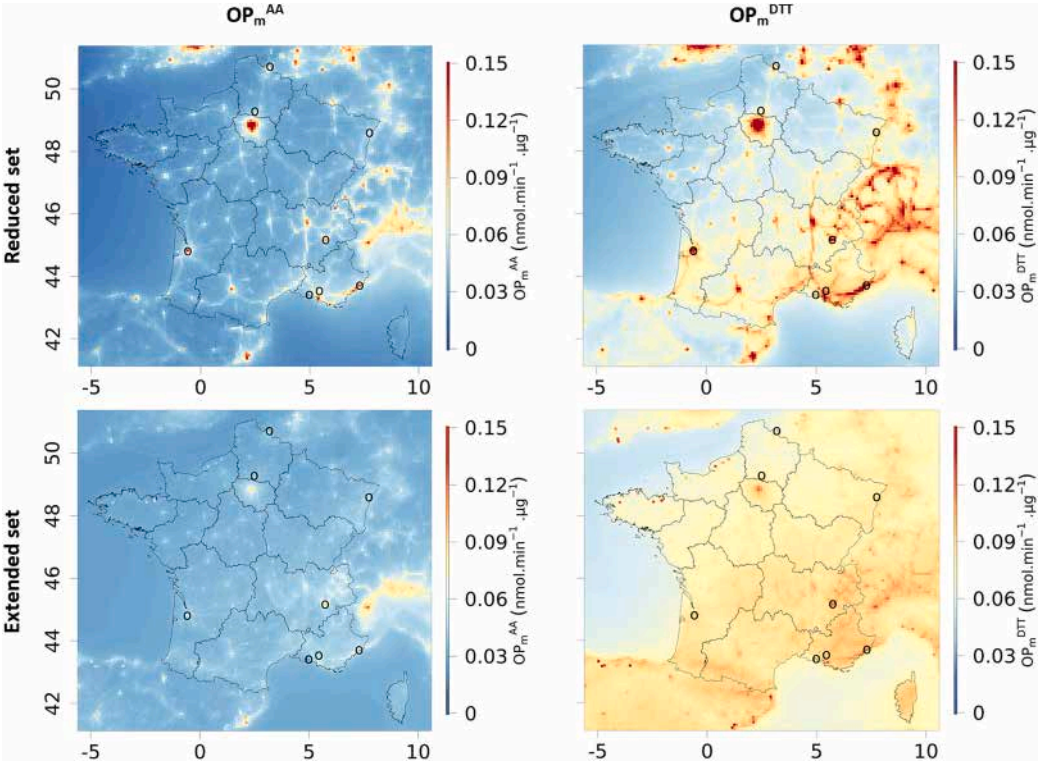

Fig. 8. Mass oxidative potential (OP_m) modelled with the reduced (top) and extended set methods (bottom) depending on the OP_m^{AA} (left) and OP_m^{DTT} (right). Biannual mean oxidative potential (2013–2014) in the first layer of the CHIMERE model. The black circles represent the OP_v measurement sites in France. Maps for seasonal variations of OP_m are in the supplement (Fig. S12 and S13).

are larger for the reduced set method, because of the large intrinsic OP_i value of primary traffic emissions. For example, in the Paris region where the differences between methods are greatest, the maps shows an $OP_v^{AA,red}$ approximately 2.5 times higher than the $OP_v^{AA,ext}$ with 5.00 and 2.00 $nmol^{AA}$ min^{-1} m^{-3} respectively. The same ratio is found between the $OP_v^{DTT,red}$ and the $OP_v^{DTT,ext}$ (respectively 8.00 and 3.00 $nmol^{DTT}$ min^{-1} m^{-3}). However, current measurements at the Paris centre station in 2023 show that the orders of magnitude of the OP values are more like 1 $nmol^{AA}$ min^{-1} m^{-3} and 2 $nmol^{DTT}$ min^{-1} m^{-3}, which is closer to the extended set method (Internal data upon request).

As a note of caution, the very "metallic" nature of non-exhaust PM, especially regarding copper is partly responsible for its high OP_i value. It is very likely that we overestimate the impact of this fraction within our model, where we consider PPM from resuspension instead of only specific concentration of copper.

Finally, the largest OP_v values are observed outside of France, but still within the domain of the study, as for example over the Po valley or the Benelux, corresponding also to large PM_{10} values simulated in these regions. In these areas, the $OP_v^{DTT,red}$ is around 8.00 $nmol^{DTT}$ min^{-1} m^{-3}, which is a high value rarely measured in Europe (Tassel et al., in prep, Grange et al., 2022).

The mass normalized oxidative potential (OP_m) results from normalising the OP_v by the PM_{10} mass concentrations. Its analysis allows highlighting regions where OP_v is not only due to higher concentrations, but also due to an increased average OP_i of its components. Fig. 8 shows the spatialization of OP_m^{AA} and OP_m^{DTT} according to the two modelling

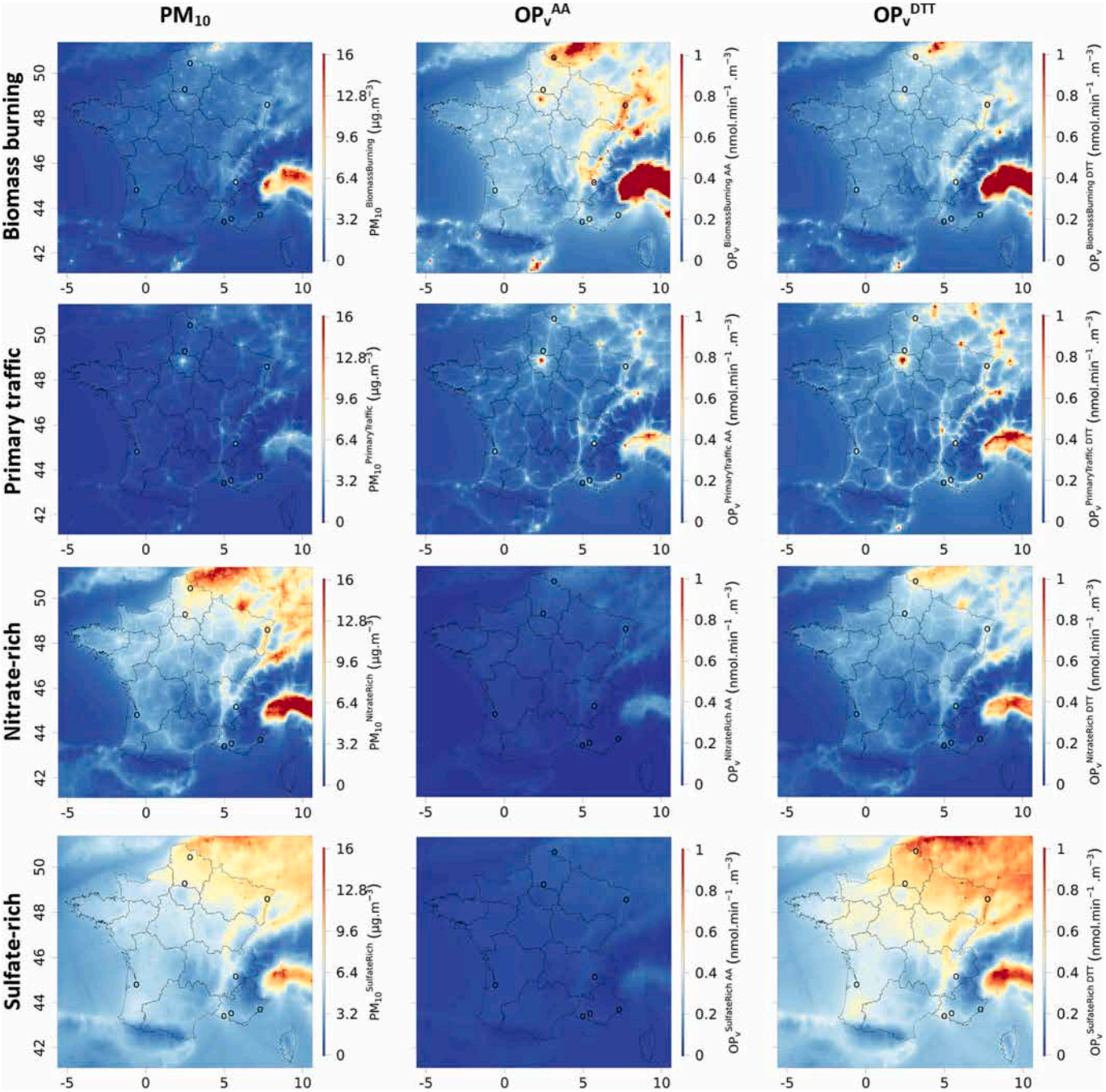

Fig. 9. Contribution of major extended set sources to PM_{10} (left), OP_v^{AA} (middle) and OP_v^{DTT} (right) spatialized over France as a two-year average (2013–2014). Only the first vertical level of the CHIMERE model is shown. Other sources contributions are in the supplement (Fig. S9).

methods.

With the reduced source set method, the OP_m^{AA} and OP_m^{DTT} are highest in densely populated areas such as the Paris region, and along major roads. In dense cities, both OP_m can be >0.10 nmol min^{-1} μg^{-1}, reflecting the fact that the potential toxicity of urban aerosols is significantly larger than in rural areas. Also, the $OP_m^{DTT,red}$ is larger overall than the AA counterpart, which can be explained by the larger and non-zero OP_i^{DTT} value for the HOA and BSOA sources.

For the extended set of sources, OP_m is still larger over urban areas with respect to rural background, but the overall distribution is more homogeneous. This is due (i) to the much lower intrinsic OP_i used for the traffic source which affects the urban agglomerations and highways, and (ii) due to a larger number of secondary sources, which are relative to the primary ones more important for rural background. As a conclusion, this analysis shows especially for the reduced set but to a lesser extent with the extended set, that urban OP_v is enhanced not only due to increased PM_{10} concentrations, but also due to increased OP_i values of urban type PM sources. OP_m appears as a good integrative metric to illustrate these effects.

4.2. Source contribution to PM and OP_v

Fig. 9 shows the contributions of the main sources to OP_v^{AA} and OP_v^{DTT} for the extended source set method averaged over two years (other sources are displayed in Fig. S9). The contribution of sources to PM_{10} concentrations appears to be different for OP_v^{AA} and OP_v^{DTT}. These maps clearly show that biomass combustion and primary traffic sources drive the levels of OP_v^{AA} and OP_v^{DTT}, especially in large cities. For OP_v^{AA}, the contribution of the other sources is negligible, while they do contribute more for OP_v^{DTT}. This is due to different intrinsic OP_i values for OP_v^{AA} and OP_v^{DTT} as pointed out in Section 2.3.

Strong differences in source contribution do appear between PM_{10} and the two tests of OP_v. These differences are particularly evident for biomass combustion and primary traffic sources, which contribute relatively less to annual total aerosol mass but significantly influence the OP_v. This observation highlights the kind of information provided by the OPv, which could be crucial in the future to help guiding policies aimed at mitigating health impacts caused by aerosols.

The contributions per source for the method based on the reduced source set have also been analysed (Fig. 10). In this approach, the abrasion source associated with road transport emerges as the most significant contributor to the oxidative potential of both AA and DTT in our study, as already shown by Daellenbach et al. (2020) with the CAMx model. By addressing and minimizing these emissions, there is a potential to substantially decrease the oxidative potential of aerosols. The disparity in the contributions of sources to PM_{10} over the French territory is even more pronounced as these sources exhibit relatively low mass contributions but high OP_v. On the contrary, the biomass combustion source is not a major contributor in this approach. Similarly, the secondary biogenic source contributes much to the PM mass, but very little to oxidative potential.

The use of these two methods, based on different PMF, introduces greater complexity into the modelling of the OP, but also illustrates the potential for refining the sources taken into account. Indeed, we see the possibility of separating exhaust and non-exhaust contributions from traffic, but also of better characterization of certain PMF factors such as nitrate and especially sulfate-rich using organic matter speciation.

5. Conclusions

This study, one of the first attempts to model Oxidative Potential on a large spatial scale, developed and tested two methods for simulating oxidative potential (OP) in a chemistry-transport model, incorporating unprecedented numerous sources and measurements. The methods complement each other: one is species-oriented, particularly for organic aerosol, and the other is source-oriented, based on chemical tracers. The study used a unique database of PM_{10} composition, source attribution, and OP_v measurements to identify uncertainties at each stage of the modelling framework. Over two years, the CHIMERE model accurately simulated PM_{10} concentrations, though with limitations in areas with complex terrain like the Alps.

The methods' ability to simulate sources obtained by PMF analysis, combined with the PSAT method (*adhoc* approach finding the correspondence between PMF and PSAT using the chemical profiles and then testing the correlation and the biases obtained by comparing the concentrations of PM linked to these sources), shows promising results. The models' OP_v simulations are encouraging but complex, especially in Mediterranean and Alpine regions. The method using a larger panel of sources correlates better with observations despite a slight bias. While the volume of data is unprecedented for this type of assessment, more data is needed in the future to cover the geographical areas investigated and the typology of sites. It will also be necessary to investigate the finer fractions of PM in terms of OP (e.g. $PM_{2.5}$, PM_1).

Key findings for both methods include higher OP_v values in urban areas, major roads, and valleys due to traffic emissions, while densely vegetated areas contribute little to OP_v. The study emphasizes the significant impact of anthropogenic sources on OP_v, suggesting that public health policies should prioritize urban areas. Road transport and biomass combustion are major contributors to OP_v, particularly in urban centers and along major roads. Extending this study to a larger European dataset of OP_i with additional sites and years could validate the methods in different environments and improve understanding of OP_v across Europe.

Finally, by focusing on reducing sources that contribute significantly to the oxidative potential in addition to PM_{10} mass, policymakers can develop more targeted and efficient mitigation measures that prioritize public health protection while accounting for regional complexities.

Acronyms

OP_v	Volume oxidative potential
OP_v^{AA}	Volume oxidative potential with ascorbic acid
OP_v^{DTT}	Volume oxidative potential with dithiothreitol
OP_i	Intrinsic oxidative potential of sources
OP_m	Mass normalized oxidative potential (OP_v/PM_{10})

CRediT authorship contribution statement

Matthieu Vida: Writing – original draft, Methodology, Investigation, Formal analysis, Conceptualization. **Gilles Foret:** Writing – review & editing, Methodology, Investigation, Funding acquisition, Conceptualization. **Guillaume Siour:** Writing – review & editing, Methodology, Investigation, Formal analysis, Conceptualization. **Jean-Luc Jaffrezo:** Writing – review & editing, Methodology, Investigation, Formal analysis, Conceptualization. **Olivier Favez:** Writing – review & editing, Methodology, Investigation, Formal analysis, Data curation. **Arineh Cholakian:** Writing – review & editing, Methodology, Formal analysis, Data curation. **Julie Cozic:** Writing – review & editing, Data curation. **Harry Dupont:** Writing – review & editing, Data curation. **Grégory Gille:** Writing – review & editing, Data curation. **Sonia Oppo:** Writing – review & editing, Data curation. **Shouwen Zhang:** Writing – review & editing, Data curation. **Florie Francony:** Writing – review & editing, Data curation. **Cyril Pallares:** Writing – review & editing, Data curation. **Sébastien Conil:** Writing – review & editing, Data curation. **Gaelle Uzu:** Writing – review & editing, Supervision, Methodology, Investigation, Formal analysis, Data curation, Conceptualization. **Matthias Beekmann:** Writing – review & editing, Supervision, Methodology, Investigation, Formal analysis, Conceptualization.

Financial support

The PhD of MV is funded by ADEME and the Paris Region in the

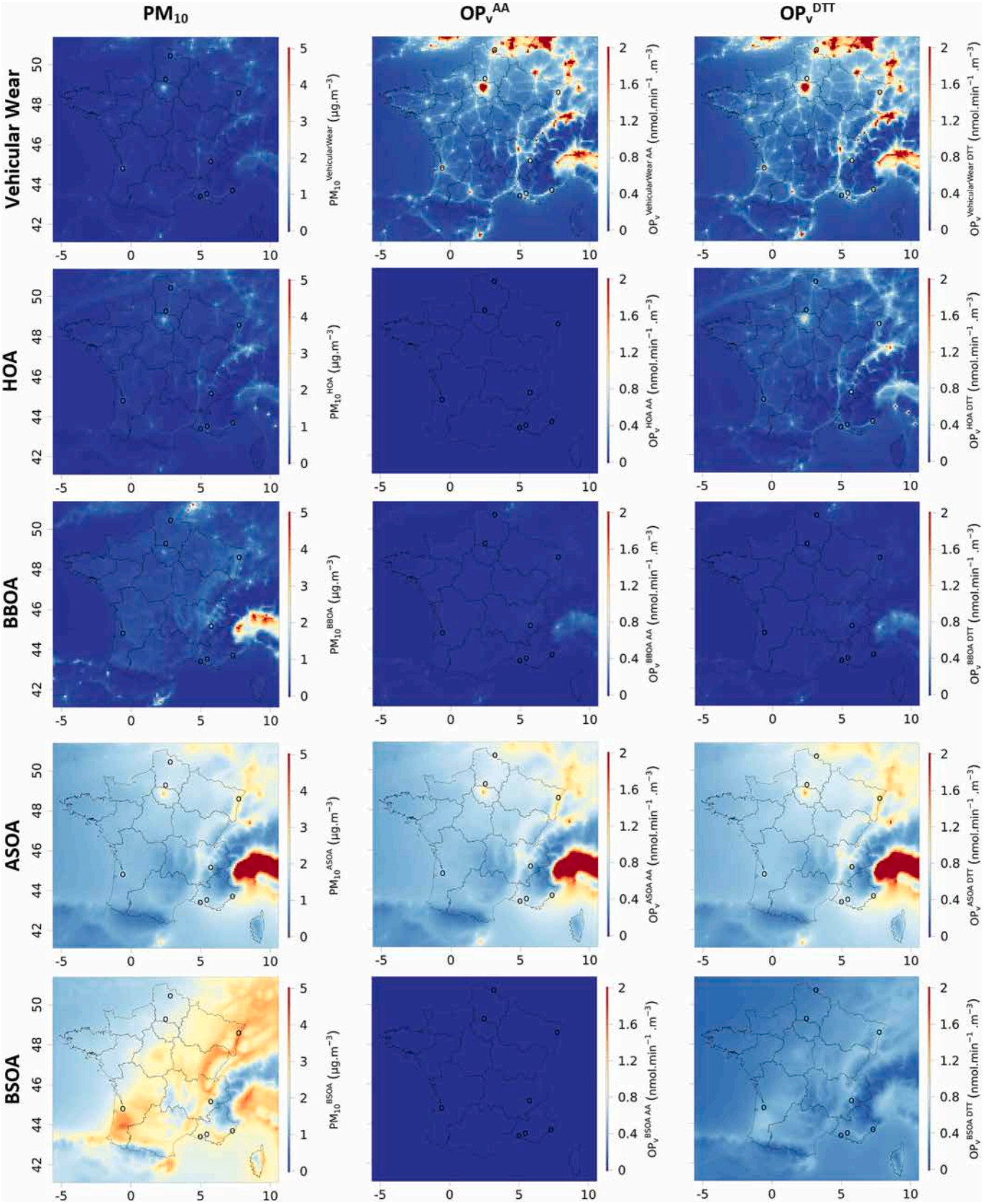

Fig. 10. Contribution of sources for the reduced set method to PM_{10} (left), OP_v^{AA} (middle) and OP_v^{DTT} (right) spatialized over France as a two-year average (2013–2014) for the reduced set of sources method. Only the first vertical level of the CHIMERE model is shown.

framework of the research network on air quality, the DIM Qi^2. This work has also been supported by the EU Horizon 2020 Green Deal project RI-URBANS (grant no. 101036245). Authors want to thank the EU project #874753 REMEDIA which currently supports the activities of M. Vida.

The ANR program "Atmospheric Biogenic Sugar" ANR-21-CE01-0021-01 provided some financial support for this collaboration, while analytical aspects were also supported at IGE by the Air-O-Sol platform within Labex OSUG@2020 (ANR10 LABX56). The work at IGE for the Andra-OPE site is supported by a long-term grant from Andra. This project was partially supported for the analytical part at IGE by the ANR project ANR GetOPstandOP ANR19-CE34-002 and Idex ACME (ANR-15-IDEX-02). The CARA program is funded the French Ministry of Environment. This work was granted access to the HPC resources of TGCC under the allocation 2022-A0130107232 made by GENCI.

Declaration of competing interest

The authors declare the following financial interests/personal relationships which may be considered as potential competing interests: Reports a relationship with that includes:. Has patent pending to. If there are other authors, they declare that they have no known competing financial interests or personal relationships that could have appeared to influence the work reported in this paper.

Acknowledgments

The authors warmly thank the dedicated work of Robin Aujay-Plouzeau (Ineris) and the numerous AQMN technicians (Atmo AuRA, Atmo Sud, Atmo HdF, Atmo GE, …) for collecting the filter samples in the field. All the many engineers and technicians on the Air O Sol analytical plateau at IGE are warmly thanked for their work at analysing the samples for the chemistry and OP. The authors also thank B. Mesbah (Atmos Sud) it's contribution to the present paper.

Appendix A. Supplementary data

Supplementary data to this article can be found online at https://doi.org/10.1016/j.scitotenv.2025.178813.

Data availability

All measurement and PMF data for this paper are archived at the IGE, and are available on request from the corresponding authors (JLJ and GU). The codes and modelling data are available from the LISA authors (MV, GF, MB, GS).

The model is available here: https://www.lmd.polytechnique.fr/chimere

References

Adélaïde, L., Medina, S., Wagner, V., de Crouy-Chanel, P., Real, E., Colette, A., Couvidat, F., Bessagnet, B., Alter, M., Durou, A., Host, S., Hulin, M., Corso, M., and Pascal, M.: Impact de la pollution de l'air ambiant sur la mortalité en France métropolitaine: réduction en lien avec le confinement du printemps 2020 et impact à long terme pour la période 2016-2019., Bull Epidémiol Hebd., 232–42, 2021.

Alleman, L.Y., Lamaison, L., Perdrix, E., Robache, A., Galloo, J.-C., 2010. PM10 metal concentrations and source identification using positive matrix factorization and wind sectoring in a French industrial zone. Atmos. Res. 96, 612–625. https://doi.org/10.1016/j.atmosres.2010.02.008.

Ayres, J.G., Borm, P., Cassee, F.R., Castranova, V., Donaldson, K., Ghio, A., Harrison, R. M., Hider, R., Kelly, F., Kooter, I.M., Marano, F., Maynard, R.L., Mudway, I., Nel, A., Sioutas, C., Smith, S., Baeza-Squiban, A., Cho, A., Duggan, S., Froines, J., 2008. Evaluating the toxicity of airborne particulate matter and nanoparticles by measuring oxidative stress potential—a workshop report and consensus statement. Inhal. Toxicol. 20, 75–99. https://doi.org/10.1080/08958370701665517.

Bates, J.T., Weber, R.J., Verma, V., Fang, T., Ivey, C., Liu, C., Sarnat, S.E., Chang, H.H., Mulholland, J.A., Russell, A., 2018. Source impact modeling of spatiotemporal trends in PM2.5 oxidative potential across the eastern United States. Atmos. Environ. 193, 158–167. https://doi.org/10.1016/j.atmosenv.2018.08.055.

Bates, J.T., Fang, T., Verma, V., Zeng, L., Weber, R.J., Tolbert, P.E., Abrams, J.Y., Sarnat, S.E., Klein, M., Mulholland, J.A., Russell, A.G., 2019. Review of acellular assays of ambient particulate matter oxidative potential: methods and relationships with composition, sources, and health effects. Environ. Sci. Technol. 53, 4003–4019. https://doi.org/10.1021/acs.est.8b03430.

Belis, C. A., Pernigotti, D., Pirovano, G., Favez, O., Jaffrezo, J. L., Kuenen, J., Denier Van Der Gon, H., Reizer, M., Riffault, V., Alleman, L. Y., Almeida, M., Amato, F., Angyal, A., Argyropoulos, G., Bande, S., Beslic, I., Besombes, J.-L., Bove, M. C., Brotto, P., Calori, G., Cesari, D., Colombi, C., Contini, D., De Gennaro, G., Di Gilio, A., Diapouli, E., El Haddad, I., Elbern, H., Eleftheriadis, K., Ferreira, J., Vivanco, M. G., Gilardoni, S., Golly, B., Hellebust, S., Hopke, P. K., Izadmanesh, Y., Jorquera, H., Krajsek, K., Kranenburg, R., Lazzeri, P., Lenartz, F., Lucarelli, F., Maciejewska, K., Manders, A., Manousakas, M., Masiol, M., Mircea, M., Mooibroek, D., Nava, S., Oliveira, D., Paglione, M., Pandolfi, M., Perrone, M., Petralia, E., Pietrodangelo, A., Pillon, S., Pokorna, P., Prati, P., Salameh, D., Samara, C., Samek, L., Saraga, D., Sauvage, S., Schaap, M., Scotto, F., Sega, K., Siour, G., Tauler, R., Valli, G., Vecchi, R., Venturini, E., Vestenius, M., Waked, A., and Yubero, E.: Evaluation of receptor and chemical transport models for PM10 source apportionment, Atmospheric Environment: X, 5, 100053, doi:https://doi.org/10.1016/j.aeaoa.2019.100053, 2020.

Bessagnet, B., Menut, L., Lapere, R., Couvidat, F., Jaffrezo, J.-L., Mailler, S., Favez, O., Pennel, R., Siour, G., 2020. High resolution chemistry transport modeling with the on-line CHIMERE-WRF model over the French Alps—analysis of a feedback of surface particulate matter concentrations on mountain meteorology. Atmosphere 11, 565. https://doi.org/10.3390/atmos11060565.

Borlaza, L.J., Weber, S., Marsal, A., Uzu, G., Jacob, V., Besombes, J.-L., Chatain, M., Conil, S., Jaffrezo, J.-L., 2022. Nine-year trends of PM $_{10}$ sources and oxidative potential in a rural background site in France. Atmos. Chem. Phys. 22, 8701–8723. https://doi.org/10.5194/acp-22-8701-2022.

Borlaza, L. J. S., Weber, S., Jaffrezo, J.-L., Houdier, S., Slama, R., Rieux, C., Albinet, A., Micallef, S., Trébluchon, C., and Uzu, G.: Disparities in particulate matter (PM10) origins and oxidative potential at a city scale (Grenoble, France) – part 2: sources of PM10 oxidative potential using multiple linear regression analysis and the predictive applicability of multilayer perceptron neural network analysis, Atmos. Chem. Phys., 21, 9719–9739, doi:https://doi.org/10.5194/acp-21-9719-2021, 2021ab.

Borlaza, L. J. S., Weber, S., Uzu, G., Jacob, V., Cañete, T., Micallef, S., Trébuchon, C., Slama, R., Favez, O., and Jaffrezo, J.-L.: Disparities in particulate matter (PM10) origins and oxidative potential at a city scale (Grenoble, France) – part 1: source apportionment at three neighbouring sites, Atmos. Chem. Phys., 21, 5415–5437, doi: https://doi.org/10.5194/acp-21-5415-2021, 2021ba.

Boylan, J.W., Russell, A.G., 2006. PM and light extinction model performance metrics, goals, and criteria for three-dimensional air quality models. Atmos. Environ. 40, 4946–4959. https://doi.org/10.1016/j.atmosenv.2005.09.087.

Brighty, A., Jacob, V., Uzu, G., Borlaza, L., Conil, S., Hueglin, C., Grange, S.K., Favez, O., Trébuchon, C., Jaffrezo, J.-L., 2022. Cellulose in atmospheric particulate matter at rural and urban sites across France and Switzerland. Atmos. Chem. Phys. 22, 6021–6043. https://doi.org/10.5194/acp-22-6021-2022.

Brook, R.D., Rajagopalan, S., Pope, C.A., Brook, J.R., Bhatnagar, A., Diez-Roux, A.V., Holguin, F., Hong, Y., Luepker, R.V., Mittleman, M.A., Peters, A., Siscovick, D., Smith, S.C., Whitsel, L., Kaufman, J.D., 2010. Particulate matter air pollution and cardiovascular disease: an update to the scientific statement from the American Heart Association. Circulation 121, 2331–2378. https://doi.org/10.1161/CIR.0b013e3181dbece1.

Calas, A., Uzu, G., Martins, J.M.F., Voisin, D., Spadini, L., Lacroix, T., Jaffrezo, J.-L., 2017. The importance of simulated lung fluid (SLF) extractions for a more relevant evaluation of the oxidative potential of particulate matter. Sci. Rep. 7, 11617. https://doi.org/10.1038/s41598-017-11979-3.

Calas, A., Uzu, G., Besombes, J.-L., Martins, J.M.F., Redaelli, M., Weber, S., Charron, A., Albinet, A., Chevrier, F., Brulfert, G., Mesbah, B., Favez, O., Jaffrezo, J.-L., 2019. Seasonal variations and chemical predictors of oxidative potential (OP) of particulate matter (PM), for seven urban French sites. Atmosphere 10, 698. https://doi.org/10.3390/atmos10110698.

Cavalli, F., Viana, M., Yttri, K.E., Genberg, J., 2010. Toward a standardised thermal-optical protocol for measuring atmospheric organic and elemental carbon: the EUSAAR protocol. Atmos. Meas. Tech. 3, 79–89. https://doi.org/10.5194/amt-3-79-2010.

Charron, A., Polo-Rehn, L., Besombes, J.-L., Golly, B., Buisson, C., Chanut, H., Marchand, N., Guillaud, G., Jaffrezo, J.-L., 2019. Identification and quantification of particulate tracers of exhaust and non-exhaust vehicle emissions. Atmos. Chem. Phys. 19, 5187–5207. https://doi.org/10.5194/acp-19-5187-2019.

Cho, A.K., Sioutas, C., Miguel, A.H., Kumagai, Y., Schmitz, D.A., Singh, M., Eiguren-Fernandez, A., Froines, J.R., 2005. Redox activity of airborne particulate matter at different sites in the Los Angeles Basin. Environ. Res. 99, 40–47. https://doi.org/10.1016/j.envres.2005.01.003.

Cholakian, A., Beekmann, M., Colette, A., Coll, I., Siour, G., Sciare, J., Marchand, N., Couvidat, F., Pey, J., Gros, V., Sauvage, S., Michoud, V., Sellegri, K., Colomb, A., Sartelet, K., Langley DeWitt, H., Elser, M., Prévot, A.S.H., Szidat, S., Dulac, F., 2018. Simulation of fine organic aerosols in the western Mediterranean area during the ChArMEx 2013 summer campaign. Atmos. Chem. Phys. 18, 7287–7312. https://doi.org/10.5194/acp-18-7287-2018.

Cholakian, A., Coll, I., Colette, A., Beekmann, M., 2021. Exposure of the population of southern France to air pollutants in future climate case studies. Atmos. Environ. 264, 118689. https://doi.org/10.1016/j.atmosenv.2021.118689.

Costabile, F., Gualtieri, M., Canepari, S., Tranfo, G., Consales, C., Grollino, M.G., Paci, E., Petralia, E., Pigini, D., Simonetti, G., 2019. Evidence of association between aerosol properties and in-vitro cellular oxidative response to PM1, oxidative potential of

PM2.5, a biomarker of RNA oxidation, and its dependency on combustion sources. Atmos. Environ. 213, 444–455. https://doi.org/10.1016/j.atmosenv.2019.06.023.
Couvidat, F., Bessagnet, B., Garcia-Vivanco, M., Real, E., Menut, L., Colette, A., 2018. Development of an inorganic and organic aerosol model (CHIMERE 2017β v1.0): seasonal and spatial evaluation over Europe. Geosci. Model Dev. 11, 165–194. https://doi.org/10.5194/gmd-11-165-2018.
Daellenbach, K.R., Kourtchev, I., Vogel, A.L., Bruns, E.A., Jiang, J., Petäjä, T., Jaffrezo, J.-L., Aksoyoglu, S., Kalberer, M., Baltensperger, U., El Haddad, I., Prévôt, A.S.H., 2019. Impact of anthropogenic and biogenic sources on the seasonal variation in the molecular composition of urban organic aerosols: a field and laboratory study using ultra-high-resolution mass spectrometry. Atmos. Chem. Phys. 19, 5973–5991. https://doi.org/10.5194/acp-19-5973-2019.
Daellenbach, K.R., Uzu, G., Jiang, J., Cassagnes, L.-E., Leni, Z., Vlachou, A., Stefenelli, G., Canonaco, F., Weber, S., Segers, A., Kuenen, J.J.P., Schaap, M., Favez, O., Albinet, A., Aksoyoglu, S., Dommen, J., Baltensperger, U., Geiser, M., El Haddad, I., Jaffrezo, J.-L., Prévôt, A.S.H., 2020. Sources of particulate-matter air pollution and its oxidative potential in Europe. Nature 587, 414–419. https://doi.org/10.1038/s41586-020-2902-8.
Dinh Ngoc Thuy, V., Jaffrezo, J.-L., Hough, I., Dominutti, P., Salque Moreton, G., Gilles, G., Francony, F., Patron-Anquez, A., Favez, O., and Uzu, G.: Unveiling the optimal regression model for source apportionment of the oxidative potential of PM, doi:https://doi.org/10.5194/egusphere-2024-361, 19 February 2024.
Dominutti, P.A., Borlaza, L.J.S., Sauvain, J.-J., Ngoc Thuy, V.D., Houdier, S., Suarez, G., Jaffrezo, J.-L., Tobin, S., Trébuchon, C., Socquet, S., Moussu, E., Mary, G., Uzu, G., 2023. Source apportionment of oxidative potential depends on the choice of the assay: insights into 5 protocols comparison and implications for mitigation measures. Environ. Sci.: Atmos. 3, 1497–1512. https://doi.org/10.1039/D3EA00007A.
Favez, O., Cachier, H., Sciare, J., Alfaro, S.C., El-Araby, T.M., Harhash, M.A., Abdelwahab, M.M., 2008. Seasonality of major aerosol species and their transformations in Cairo megacity. Atmos. Environ. 42, 1503–1516. https://doi.org/10.1016/j.atmosenv.2007.10.081.
Favez, O., El Haddad, I., Piot, C., Boréave, A., Abidi, E., Marchand, N., Jaffrezo, J.-L., Besombes, J.-L., Personnaz, M.-B., Sciare, J., Wortham, H., George, C., D'Anna, B., 2010. Inter-comparison of source apportionment models for the estimation of wood burning aerosols during wintertime in an Alpine city (Grenoble, France). Atmos. Chem. Phys. 10, 5295–5314. https://doi.org/10.5194/acp-10-5295-2010.
Favez, O., Weber, S., Petit, J.-E., Alleman, L.Y., Albinet, A., Riffault, V., Chazeau, B., Amodeo, T., Salameh, D., Zhang, Y., Srivastava, D., Samaké, A., Aujay-Plouzeau, R., Papin, A., Bonnaire, N., Boullanger, C., Chatain, M., Chevrier, F., Detournay, A., Dominik-Sègue, M., Falhun, R., Garbin, C., Ghersi, V., Grignion, G., Levigoureux, G., Pontet, S., Rangognio, J., Zhang, S., Besombes, J.-L., Conil, S., Uzu, G., Savarino, J., Marchand, N., Gros, V., Marchand, C., Jaffrezo, J.-L., Leoz-Garziandia, E., 2021. Overview of the French operational network for in situ observation of PM chemical composition and sources in urban environments (CARA program). Atmosphere 12, 207. https://doi.org/10.3390/atmos12020207.
Font, A., Brito, J.-F., Riffault, V., Conil, S., Jaffrezo, J.-L., Sauvage, S., Bourin, A., 2024. Long–term measurements of aerosol composition at rural background sites in France: sources, seasonality and mass closure of $PM_{2.5}$. Atmos. Environ. 334, 120724. https://doi.org/10.1016/j.atmosenv.2024.120724. ISSN 1352-2310.
Fortems-Cheiney, A., Foret, G., Siour, G., Vautard, R., Szopa, S., Dufour, G., Colette, A., Lacressonniere, G., Beekmann, M., 2017. A 3 °C global RCP8.5 emission trajectory cancels benefits of European emission reductions on air quality. Nat. Commun. 8, 89. https://doi.org/10.1038/s41467-017-00075-9.
Fortems-Cheiney, A., Dufour, G., Dufossé, K., Couvidat, F., Gilliot, J.-M., Siour, G., Beekmann, M., Foret, G., Meleux, F., Clarisse, L., Coheur, P.-F., Van Damme, M., Clerbaux, C., Génermont, S., 2020. Do alternative inventories converge on the spatiotemporal representation of spring ammonia emissions in France? Atmos. Chem. Phys. 20, 13481–13495. https://doi.org/10.5194/acp-20-13481-2020.
Gao, D., Ripley, S., Weichenthal, S., and Godri Pollitt, K. J.: Ambient particulate matter oxidative potential: Chemical determinants, associated health effects, and strategies for risk management, Free Radical Biology and Medicine, 151, 7–25, doi:https://doi.org/10.1016/j.freeradbiomed.2020.04.028, 2020.
Grange, S.K., Uzu, G., Weber, S., Jaffrezo, J.-L., Hueglin, C., 2022. Linking Switzerland's PM_{10} and $PM_{2.5}$ oxidative potential (OP) with emission sources. Atmos. Chem. Phys. 22, 7029–7050. https://doi.org/10.5194/acp-22-7029-2022.
Guenther, A.B., Jiang, X., Heald, C.L., Sakulyanontvittaya, T., Duhl, T., Emmons, L.K., Wang, X., 2012. The Model of Emissions of Gases and Aerosols from Nature version 2.1 (MEGAN2.1): an extended and updated framework for modeling biogenic emissions. Geosci. Model Dev. 5, 1471–1492. https://doi.org/10.5194/gmd-5-1471-2012.
Heald, C.L., Spracklen, D.V., 2009. Atmospheric budget of primary biological aerosol particles from fungal spores. Geophys. Res. Lett. 36, 2009GL037493. https://doi.org/10.1029/2009GL037493.
Inness, A., Ades, M., Agustí-Panareda, A., Barré, J., Benedictow, A., Blechschmidt, A.-M., Dominguez, J.J., Engelen, R., Eskes, H., Flemming, J., Huijnen, V., Jones, L., Kipling, Z., Massart, S., Parrington, M., Peuch, V.-H., Razinger, M., Remy, S., Schulz, M., Suttie, M., 2019. The CAMS reanalysis of atmospheric composition. Atmos. Chem. Phys. 19, 3515–3556. https://doi.org/10.5194/acp-19-3515-2019.
Jaffrezo, J.-L., Aymoz, G., Delaval, C., Cozic, J., 2005. Seasonal variations of the water soluble organic carbon mass fraction of aerosol in two valleys of the French Alps. Atmos. Chem. Phys. 5, 2809–2821. https://doi.org/10.5194/acp-5-2809-2005.
Karavalakis, G., Gysel, N., Schmitz, D.A., Cho, A.K., Sioutas, C., Schauer, J.J., Cocker, D. R., Durbin, T.D., 2017. Impact of biodiesel on regulated and unregulated emissions, and redox and proinflammatory properties of PM emitted from heavy-duty vehicles. Sci. Total Environ. 584–585, 1230–1238. https://doi.org/10.1016/j.scitotenv.2017.01.187.
Lelieveld, J., Evans, J.S., Fnais, M., Giannadaki, D., Pozzer, A., 2015. The contribution of outdoor air pollution sources to premature mortality on a global scale. Nature 525, 367–371. https://doi.org/10.1038/nature15371.
Leni, Z., Cassagnes, L.E., Daellenbach, K.R., El Haddad, I., Vlachou, A., Uzu, G., Prévôt, A.S.H., Jaffrezo, J.-L., Baumlin, N., Salathe, M., Baltensperger, U., Dommen, J., Geiser, M., 2020. Oxidative stress-induced inflammation in susceptible airways by anthropogenic aerosol. PloS One 15, e0233425. https://doi.org/10.1371/journal.pone.0233425.
Li, Q., Wyatt, A., Kamens, R.M., 2009. Oxidant generation and toxicity enhancement of aged-diesel exhaust. Atmos. Environ. 43, 1037–1042. https://doi.org/10.1016/j.atmosenv.2008.11.018.
Liu, Q., Baumgartner, J., Zhang, Y., Liu, Y., Sun, Y., Zhang, M., 2014. Oxidative potential and inflammatory impacts of source apportioned ambient air pollution in Beijing. Environ. Sci. Technol. 48 (21), 12920–12929. https://doi.org/10.1021/es5029876.
Loosmore, G.A., 2003. Evaluation and development of models for resuspension of aerosols at short times after deposition. Atmos. Environ. 37, 639–647. https://doi.org/10.1016/S1352-2310(02)00902-0.
Marécal, V., Peuch, V.-H., Andersson, C., Andersson, S., Arteta, J., Beekmann, M., Benedictow, A., Bergström, R., Bessagnet, B., Cansado, A., Chéroux, F., Colette, A., Coman, A., Curier, R. L., Denier Van Der Gon, H. A. C., Drouin, A., Elbern, H., Emili, E., Engelen, R. J., Eskes, H. J., Foret, G., Friese, E., Gauss, M., Giannaros, C., Guth, J., Joly, M., Jaumouillé, E., Josse, B., Kadygrov, N., Kaiser, J. W., Krajsek, K., Kuenen, J., Kumar, U., Liora, N., Lopez, E., Malherbe, L., Martinez, I., Melas, D., Meleux, F., Menut, L., Moinat, P., Morales, T., Parmentier, J., Piacentini, A., Plu, M., Poupkou, A., Queguiner, S., Robertson, L., Rouïl, L., Schaap, M., Segers, A., Sofiev, M., Tarasson, L., Thomas, M., Timmermans, R., Valdebenito, Á., Van Velthoven, P., Van Versendaal, R., Vira, J., and Ung, A.: A regional air quality forecasting system over Europe: the MACC-II daily ensemble production, Geosci. Model Dev., 8, 2777–2813, doi:https://doi.org/10.5194/gmd-8-2777-2015, 2015.
Mareckova, K., Pinterits, M., Ullrich, B., Wankmueller, R., and Mandl, N.: Review of emission data reported under the LRTAP Convention and NEC Directive Centre Emission Inventories Project, Technical Report 4/2018, CEIP, https://www.ceip.at/fileadmin/inhalte/ceip/00_pdf_other/2018/inventoryreport_2018.pdf, (last access: 10 June 2024), 2018.
Marsal, A., Sauvain, J.-J., Thomas, A., Lyon-Caen, S., Borlaza, L.J.S., Philippat, C., Jaffrezo, J.-L., Boudier, A., Darfeuil, S., Elazzouzi, R., Lepeule, J., Chartier, R., Bayat, S., Slama, R., Siroux, V., Uzu, G., 2024. Effects of personal exposure to the oxidative potential of PM2.5 on oxidative stress biomarkers in pregnant women. Sci. Total Environ. 911, 168475. https://doi.org/10.1016/j.scitotenv.2023.168475.
Mbengue, S., Alleman, L.Y., Flament, P., 2014. Size-distributed metallic elements in submicronic and ultrafine atmospheric particles from urban and industrial areas in northern France. Atmos. Res. 135–136, 35–47. https://doi.org/10.1016/j.atmosres.2013.08.010.
Menut, L., Bessagnet, B., Briant, R., Cholakian, A., Couvidat, F., Mailler, S., Pennel, R., Siour, G., Tuccella, P., Turquety, S., Valari, M., 2021. The CHIMERE v2020r1 online chemistry-transport model. Geosci. Model Dev. 14, 6781–6811. https://doi.org/10.5194/gmd-14-6781-2021.
NCEP, 2000. NCEP FNL Operational Model Global Tropospheric Analyses, Continuing from July 1999. https://doi.org/10.5065/D6M043C6.
Paatero, P., Tapper, U., 1994. Positive matrix factorization: a non-negative factor model with optimal utilization of error estimates of data values. Environmetrics 5, 111–126. https://doi.org/10.1002/env.3170050203.
Park, M., Joo, H.S., Lee, K., Jang, M., Kim, S.D., Kim, I., Borlaza, L.J.S., Lim, H., Shin, H., Chung, K.H., Choi, Y.-H., Park, S.G., Bae, M.-S., Lee, J., Song, H., Park, K., 2018. Differential toxicities of fine particulate matters from various sources. Sci. Rep. 8, 17007. https://doi.org/10.1038/s41598-018-35398-0.
Petit, J.-E., Favez, O., Sciare, J., Crenn, V., Sarda-Estève, R., Bonnaire, N., Močnik, G., Dupont, J.-C., Haeffelin, M., Leoz-Garziandia, E., 2015. Two years of near real-time chemical composition of submicron aerosols in the region of Paris using an Aerosol Chemical Speciation Monitor (ACSM) and a multi-wavelength Aethalometer. Atmos. Chem. Phys. 15, 2985–3005. https://doi.org/10.5194/acp-15-2985-2015.
Pignon, B., Borel, C., Lajnef, M., Richard, J.-R., Szöke, A., Hemery, F., Leboyer, M., Foret, G., Schürhoff, F., 2022. PM2.5 and PM10 air pollution peaks are associated with emergency department visits for psychotic and mood disorders. Environ. Sci. Pollut. Res. 29, 88577–88586. https://doi.org/10.1007/s11356-022-21964-7.
Rienda, I.C., Alves, C.A., 2021. Road dust resuspension: a review. Atmos. Res. 261, 105740. https://doi.org/10.1016/j.atmosres.2021.105740. ISSN 0169-8095.
Rouil, L., Honoré, C., Vautard, R., Beekmann, M., Bessagnet, B., Malherbe, L., Meleux, F., Dufour, A., Elichegaray, C., Flaud, J.-M., Menut, L., Martin, D., Peuch, A., Peuch, V.-H., Poisson, N., 2009. Prev'air: an operational forecasting and mapping system for air quality in Europe. Bull. Amer. Meteor. Soc. 90, 73–84. https://doi.org/10.1175/2008BAMS2390.1.
Samaké, A., Uzu, G., Martins, J.M.F., Calas, A., Vince, E., Parat, S., Jaffrezo, J.L., 2017. The unexpected role of bioaerosols in the oxidative potential of PM. Sci. Rep. 7, 10978. https://doi.org/10.1038/s41598-017-11178-0.
Samaké, A., Jaffrezo, J.-L., Favez, O., Weber, S., Jacob, V., Albinet, A., Riffault, V., Perdrix, E., Waked, A., Golly, B., Salameh, D., Chevrier, F., Oliveira, D. M., Bonnaire, N., Besombes, J.-L., Martins, J. M. F., Conil, S., Guillaud, G., Mesbah, B., Rocq, B., Robic, P.-Y., Hulin, A., Le Meur, S., Descheemaecker, M., Chretien, E., Marchand, N., and Uzu, G.: Polyols and glucose particulate species as tracers of primary biogenic organic aerosols at 28 French sites, Atmos. Chem. Phys., 19, 3357–3374, doi: https://doi.org/10.5194/acp-19-3357-2019, 2019ab.
Samaké, A., Jaffrezo, J.-L., Favez, O., Weber, S., Jacob, V., Canete, T., Albinet, A., Charron, A., Riffault, V., Perdrix, E., Waked, A., Golly, B., Salameh, D., Chevrier, F.,

Oliveira, D. M., Besombes, J.-L., Martins, J. M. F., Bonnaire, N., Conil, S., Guillaud, G., Mesbah, B., Rocq, B., Robic, P.-Y., Hulin, A., Le Meur, S., Descheemaecker, M., Chretien, E., Marchand, N., and Uzu, G.: Arabitol, mannitol, and glucose as tracers of primary biogenic organic aerosol: the influence of environmental factors on ambient air concentrations and spatial distribution over France, Atmos. Chem. Phys., 19, 11013–11030, doi:https://doi.org/10.5194/acp-19-11013-2019, 2019ba.

Sauvain, J.-J., Deslarzes, S., Riediker, M., 2008. Nanoparticle reactivity toward dithiothreitol. Nanotoxicology 2, 121–129. https://doi.org/10.1080/17435390802245716.

Schaap, M., Van Loon, M., Ten Brink, H.M., Dentener, F.J., Builtjes, P.J.H., 2004. Secondary inorganic aerosol simulations for Europe with special attention to nitrate. Atmos. Chem. Phys. 4, 857–874. https://doi.org/10.5194/acp-4-857-2004.

Skamarock, W.C., Klemp, J.B., Dudhia, J., Gill, D.O., Barker, D.M., Duda, M.G., Huang, X.-Y., Wang, W., Powers, J.G., 2008. A Description of the Advanced Research WRF Version 3. National Center for Atmospheric Research Boulder, Colorado, USA.

Steenhof, M., Gosens, I., Strak, M., Godri, K.J., Hoek, G., Cassee, F.R., Mudway, I.S., Kelly, F.J., Harrison, R.M., Lebret, E., Brunekreef, B., Janssen, N.A., Pieters, R.H., 2011. In vitro toxicity of particulate matter (PM) collected at different sites in the Netherlands is associated with PM composition, size fraction and oxidative potential - the RAPTES project. Part. Fibre Toxicol. 8, 26. https://doi.org/10.1186/1743-8977-8-26.

Verlhac, S., Favez, O., Albinet, A., 2013. Interlaboratory comparison organized for the European laboratories involved in the analysis of levoglucosan and its isomers. https://doi.org/10.13140/RG.2.2.16262.47684.

Verma, V., Fang, T., Guo, H., King, L., Bates, J.T., Peltier, R.E., Edgerton, E., Russell, A. G., Weber, R.J., 2014. Reactive oxygen species associated with water-soluble PM2.5 in the southeastern United States: spatiotemporal trends and source apportionment. Atmos. Chem. Phys. 14, 12915–12930. https://doi.org/10.5194/acp-14-12915-2014.

Vida, M., Foret, G., Siour, G., Couvidat, F., Favez, O., Uzu, G., Cholakian, A., Conil, S., Beekmann, M., Jaffrezo, J.-L., 2024. Modelling of Atmospheric Concentrations of Fungal Spores: A Two-Year Simulation over France Using CHIMERE, EGUsphere [Preprint]. https://doi.org/10.5194/egusphere-2024-698.

Wagstrom, K.M., Pandis, S.N., Yarwood, G., Wilson, G.M., Morris, R.E., 2008. Development and application of a computationally efficient particulate matter apportionment algorithm in a three-dimensional chemical transport model. Atmos. Environ. 42, 5650–5659. https://doi.org/10.1016/j.atmosenv.2008.03.012.

Waked, A., Favez, O., Alleman, L.Y., Piot, C., Petit, J.-E., Delaunay, T., Verlinden, E., Golly, B., Besombes, J.-L., Jaffrezo, J.-L., Leoz-Garziandia, E., 2014. Source apportionment of PM10 in a north-western Europe regional urban background site (Lens, France) using positive matrix factorization and including primary biogenic emissions. Atmos. Chem. Phys. 14, 3325–3346. https://doi.org/10.5194/acp-14-3325-2014.

Weber, S., Uzu, G., Calas, A., Chevrier, F., Besombes, J.-L., Charron, A., Salameh, D., Ježek, I., Močnik, G., Jaffrezo, J.-L., 2018. An apportionment method for the oxidative potential of atmospheric particulate matter sources: application to a one-year study in Chamonix, France. Atmos. Chem. Phys. 18, 9617–9629. https://doi.org/10.5194/acp-18-9617-2018.

Weber, S., Salameh, D., Albinet, A., Alleman, L.Y., Waked, A., Besombes, J.-L., Jacob, V., Guillaud, G., Meshbah, B., Rocq, B., Hulin, A., Dominik-Sègue, M., Chrétien, E., Jaffrezo, J.-L., Favez, O., 2019. Comparison of PM10 sources profiles at 15 French sites using a harmonized constrained positive matrix factorization approach. Atmosphere 10, 310. https://doi.org/10.3390/atmos10060310.

Weber, S., Uzu, G., Favez, O., Borlaza, L.J., Calas, A., Salameh, D., Chevrier, F., Allard, J., Besombes, J.-L., Albinet, A., Pontet, S., Mesbah, B., Gille, G., Zhang, S., Pallares, C., Leoz-Garziandia, E., Jaffrezo, J.-L., 2021. Source apportionment of atmospheric PM10 oxidative potential: synthesis of 15 year-round urban datasets in France. Atmos. Chem. Phys. 21, 11353–11378. https://doi.org/10.5194/acp-21-11353-2021.

Weichenthal, S., Hoppin, J.A., Reeves, F., 2014. Obesity and the cardiovascular health effects of fine particulate air pollution. Obesity 22, 1580–1589. https://doi.org/10.1002/oby.20748.

Weichenthal, S., Lavigne, E., Evans, G., Pollitt, K., Burnett, R.T., 2016. Ambient PM2.5 and risk of emergency room visits for myocardial infarction: impact of regional PM2.5 oxidative potential: a case-crossover study. Environ. Health 15, 46. https://doi.org/10.1186/s12940-016-0129-9.

WHO, 2021. WHO Global Air Quality Guidelines: Particulate Matter (PM2.5 and PM10), Ozone, Nitrogen Dioxide, Sulfur Dioxide and Carbon Monoxide. WHO European Centre for Environment and Health, Bonn, Germany.

Yttri, K.E., Schnelle-Kreis, J., Maenhaut, W., Abbaszade, G., Alves, C., Bjerke, A., Bonnier, N., Bossi, R., Claeys, M., Dye, C., Evtyugina, M., García-Gacio, D., Hillamo, R., Hoffer, A., Hyder, M., Iinuma, Y., Jaffrezo, J.-L., Kasper-Giebl, A., Kiss, G., López-Mahia, P.L., Pio, C., Piot, C., Ramirez-Santa-Cruz, C., Sciare, J., Teinilä, K., Vermeylen, R., Vicente, A., Zimmermann, R., 2015. An intercomparison study of analytical methods used for quantification of levoglucosan in ambient aerosol filter samples. Atmos. Meas. Tech. 8, 125–147. https://doi.org/10.5194/amt-8-125-2015.